Deutsches Zentrum
für Luft- und Raumfahrt e.V.
in der Helmholtz-Gemeinschaft

EnMAP Ground Segment

Mission Quarterly Report #13

01.07.2025 to 30.09.2025

Restriction: public

Doc. ID	EN-GS-RPT-1113
Issue	1.0
Date	12.12.2025

Configuration Controlled: Yes

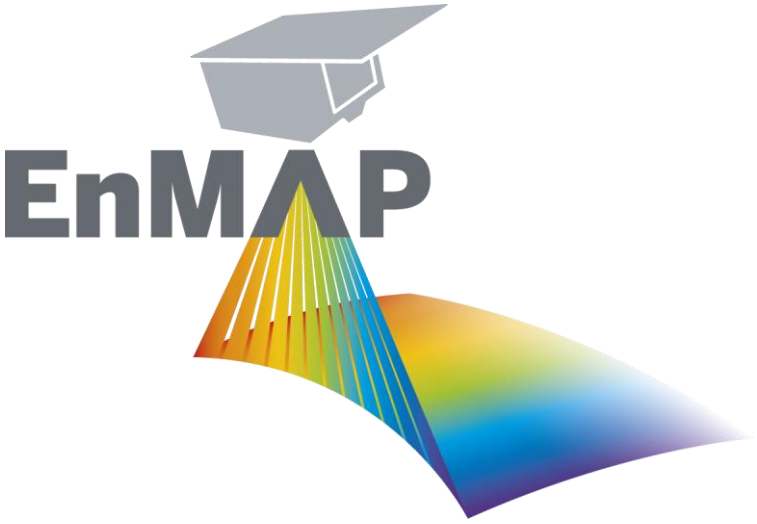

German Remote Sensing Data Center (DFD)
Remote Sensing Technology Institute (IMF)
German Space Operations Center (GSOC)
Helmholtz Centre for Geosciences (GFZ)
German Space Agency at DLR

TABLE OF SIGNATURES

Prepared	Emiliano Carmona Flores Digitally signed by Emiliano Carmona Flores DN: PostalCode=51147, O=Deutsches Zentrum fuer Luft- und Raumfahrt e. V. (DLR), STREET=Linder Höhe, S=Nordrhein-Westfalen, C=DE, CN=Emiliano Carmona Flores, E=emiliano.carmona@dlr.de Reason: I am the author of this document Location: Date: 2025.12.17 11:47:35+01'00' Foxit PDF Reader Version: 2025.2.1	
Date	Emiliano Carmona, (DLR MF-ASP, EnMAP OMM)	
	Sabine Chabrillat Digital unterschrieben von Sabine Chabrillat Datum: 2026.01.07 10:28:40 +01'00'	
Date	Sabine Chabrillat, (GFZ, EnMAP SciLead)	
Reviewed	D. Schulze Digital signiert von Daniel Schulze Datum: 2026.01.08 08:41:01+01'00'	
Date	Daniel Schulze, (DLR RB-MIB, dep. EnMAP OMM)	
	Sabine Engelbrecht Digital signiert von Sabine Engelbrecht DN: PostalCode=51147, O=Deutsches Zentrum fuer Luft- und Raumfahrt e. V. (DLR), STREET=Linder Höhe, S=Nordrhein-Westfalen, C=DE, CN=Sabine Engelbrecht, E=sabine.engelbrecht@dlr.de Grund: Ich habe dieses Dokument geprüft Ort: DLR Oberpfaffenhofen Datum: 2026.01.08 09:12:23+01'00' Foxit PDF Editor Version: 14.0.1	
Date	Sabine Engelbrecht, (DLR DFD-INF, EOC PAD)	
	Robert Größel Digital signiert von Robert Größel DN: PostalCode=51147, O=Deutsches Zentrum fuer Luft- und Raumfahrt e. V. (DLR), STREET=Linder Höhe, S=Nordrhein-Westfalen, C=DE, CN=Robert Größel, E=robert.groessel@dlr.de Grund: Ich bin der Verfasser dieses Dokuments Ort: Datum: 2026.01.08 08:19:34+01'00' Foxit PDF Reader Version: 2025.2.1	
Date	Robert Größel, (DLR RB-CTA, GSOC PAD)	
	Karl Segl Digital unterschrieben von Karl Segl Datum: 2026.01.07 10:18:38 +01'00'	
Date	Karl Segl, (GFZ, dep. EnMAP SciLead)	
Approved & Released	i.A. Laura La Porta 2026.01.08 11:11:40+01'00' 14.0.1	
Date	Laura La Porta, (DLR AR-AO, EnMAP MM)	

DISTRIBUTION LIST

The document is publicly available via www.enmap.org.

CHANGE RECORD

Version	Date	Chapter	Comment
1.0	12.12.2025	All	First issue of Mission Quarterly Report #13 corresponding to 01.07.2025 to 30.09.2025.

Custodian of this document is Carmona, Emiliano.

CONTENTS

LIST OF FIGURES

LIST OF TABLES

1 Introduction

1.1 Purpose

This mission quarterly report (MQR) states information on the EnMAP mission status with regard to the registered user community, announcements-of-opportunities and observations as well as the status of the user interfaces, satellite (platform and payload), ground stations (S-band and X-band), processor (Archive, Level 1B, Level 1C, Level 2A (land and water)), calibration (spectral, radiometric, geometric), data quality control and validation of EnMAP.

Please visit www.enmap.org for further information on EnMAP.

1.2 Scope

This 13th Mission Quarterly Report (MQR) applies to the operations of EnMAP in the reporting period of Routine Phase (RP) from **01.07.2025 to 30.09.2025 (Q3 2025)**.

2 References

Reference Identifier	Document Identifier and Title
[1]	L. Guanter et al. (2015) The EnMAP Spaceborne Imaging Spectroscopy Mission for Earth Observation. Remote Sensing, Issue 7, pp. 8830-8857.
[2]	EN-GS-UM-6020 Portals User Manual, Version 1.4
[3]	EN-PCV-ICD-2009-2 Product Specification, Version 1.9
[4]	EN-PCV-TN-4006 Level 1B ATBD, Version 1.10
[5]	EN-PCV-TN-5006 Level 1C ATBD, Version 1.7
[6]	EN-PCV-TN-6007 Level 2A (land) ATBD, Version 2.4
[7]	EN-PCV-TN-6008 Level 2A (water) ATBD, Version 3.1
[8]	Chabrillat, S. et al. (2022) EnMAP Science Plan. EnMAP Technical Report, DOI: 10.48440/enmap.2022.001
[9]	Storch, T.; Honold, H.-P.; Chabrillat, et al. The EnMAP imaging spectroscopy mission towards operations. Remote Sens. Environ. 2023, 294, 113632. DOI: 10.1016/j.rse.2023.113632

Table 2-1 References

3 Terms, Definitions and Abbreviations

Terms, definitions and abbreviations for EnMAP are collected in a database which is publicly accessible via Internet on www.enmap.org.

An Earth observation of swath length *n* × 30 km (and swath width 30 km) is separated into *n* tiles of size 30 km × 30 km.

4 Mission

4.1 Mission Objectives

The primary goal of EnMAP (Environmental Mapping and Analysis Program) is to measure, derive and analyze quantitative diagnostic parameters describing key processes on the Earth's surface [1].

During the mission operations, with the successful launch on 1st of April 2022 and an expected operational mission lifetime of at least 5 years, EnMAP will provide valuable information for various application fields comprising soil and geology, agriculture, forestry, urban areas, aquatic systems, ecosystem transitions.

4.2 Mission Description

The major elements of the EnMAP mission are the EnMAP Space Segment, built by OHB System AG and owned by the German Space Agency at DLR, the EnMAP Ground Segment built and operated by DLR institutes DFD, MF, RB, and the EnMAP User and Science Segment represented by GFZ. The project management of the EnMAP mission is responsibility of the German Space Agency at DLR.

The EnMAP Space Segment is composed of

- the platform providing power and thermal stability, orbit and attitude control, memory, S-band uplink/downlink for TM/TC data transmission/reception, X-band downlink for payload data transmission, and

- the payload realized as a pushbroom imaging dual-spectrometer covering the wavelength range between 420 nm and 2450 nm with a nominal spectral resolution ≤ 10 nm and allows in combination with a high radiometric resolution and stability to measure subtle reflectance changes.

The EnMAP satellite is operated on a sun-synchronous repeat orbit to observe any location on the globe with comparable illumination conditions. This allows a maximum reflected solar input radiance at the sensor with an acceptable risk for cloud coverage.

The EnMAP Ground Segment is the interface between Space Segment and User and Science Segment. It comprises functionalities to

- perform planning of imaging, communication and orbit maneuver operations, provision of orbit and attitude data, command and control of the satellite, ground station networks (in particular: Weilheim, Germany, for S-band and Neustrelitz, Germany, for X-Band), receive satellite data, perform long-term archiving and delivery of products, and

- perform processing chain (for systematic and radiometric correction, orthorectification, atmospheric compensation), instrument calibration operations, and the data quality control of the products.

The EnMAP mission interfaces to the international science and user community through the EnMAP Portal www.enmap.org with official information related to EnMAP by DLR and GFZ-Potsdam (as the document in hand) and links for ordering observations and products.

The EnMAP Science Segment is represented by the EnMAP Science Advisory Group chaired by the mission principal investigator at the GFZ-Potsdam. The Science Segment addresses aspects such as

- supporting and performing validation activities to improve sensor performance and product quality

- developing scientific and application research to fully exploit the scientific potential of EnMAP [8] including provision of software tools for EnMAP data processing and analyses (EnMAP-Box) and provision of teaching and education materials (HYPERedu)

- Organizing workshops, summer schools and in general information, training and networking activities for the user community

The EnMAP User Segment is the community of German and international users ordering acquisitions and accessing products of EnMAP.

4.3 Mission Status Summary

The mission successfully finished the commissioning phase (CP) on 01.11.2022 [9] and entered its routine phase (RP) on 02.11.2022. In the reporting period, from 01.07.2025 to 30.09.2025, there have been no major issues affecting the instrument or the satellite, only some minor issues have caused the loss of a small fraction of observation time.

During the period 01.07.2025 to 30.09.2025 (92 days in total), only two issues resulted in several hours of no acquisitions. One issue was caused by a HSI SAFE_ERRORs (07.08.2025), that resulted in no observations during 23 hours. Another issue was caused by a DSHA SAFETY mode (29.09.2025) that also resulted in no observations during 27 hours. In all cases the data quality is analyzed after resuming operations and no effect was found on the newly acquired data. During normal operations, the mission is regularly surpassing the initially planned maximum acquisition capacity of 5000 km / day.

In this period, 2176 Earth observations of 30 km swath width and up to 990 km swath length were successfully performed which resulted in 20625 archived Earth observation tiles of 30 km × 30 km and 27 calibration acquisitions. In addition, 14256 products were delivered from catalog orders. In total, 19765 Earth observations were performed until 30.09.2025 by the EnMAP team and the 4407 registered users with at least one active user role. This results in 174626 archived Earth observation images (214711 products including the different versions of the re-processed products) and 322413 Earth products delivered from observations requests (180351) and catalogue orders (142062) since the start of the mission. More details are presented in sections 5 and 6.

No major limitations are applicable at 30.09.2025. For minor limitations affecting data processing, check section 7.4. Other effects observed in the data by our Quality Control team are reported in section 7.6 where they are investigated in more detail.

Activities within the EnMAP Mission and in particular the Ground Segment are periodically reported in conferences and workshops. More details are available in Section 9.

The following changes were implemented in the reporting period:

- Reprocessing of L0 products to L2A ARD products with latest processor version **V01.05.02** started in September 2025. ARD products currently available with versions prior to V01.05.02 in the EO-Geoservice and EOLab platforms will be replaced by V01.05.02 along the upcoming months. During this re-processing, L1B and L1C ARD products for the complete EnMAP archive will also be generated and made available along 2026.
- Since July 2025, it is possible to access the EOC-Geoservice with the IPP (Instrument Planning Portal) user credentials. This updated access service replaces the need to create a separate EnMAP account on EOC-Geoservice to only download EnMAP data if an account on IPP exists (see section 6.2.1).

The EnMAP processor version did not change during the reporting period and it is still V01.05.02. The list of changes introduced in this and previous processor updates is available at:

https://www.enmap.org/data/doc/EnMAP_processor_changelog.pdf

Since August 2024, EnMAP L2A ARD products have been available for download through the EOC Geoservice (https://geoservice.dlr.de/) and the EO-Lab platform (https://eo-lab.org/). These possibilities allow the direct download of EnMAP L2A products generated by the EnMAP Ground Segment with a standard set of parameters. Since these L2A products are already processed, users can directly download these products without waiting times, allowing a fast way to get large amounts of EnMAP products from the mission archive. Notice that both EOC Geoservice and EO-Lab are not part of the standard services offered

by the EnMAP mission but are accessible with the GS/IPS EnMAP account. More information on the number of products downloaded through Geoservice can be found in section 6.2.1.

The following changes are expected to be performed in the next quarters:

- Implementation of new linearity calibration (and updated calibration) to improve the VNIR-SWIR matching between spectrometers, specially at low radiances.
- New processor version (**V01.05.05**). For more details on this new version see section 7.4.

5 Users and Announcements-of-Opportunities

5.1 Users

	Country/Continent (No of Countries) *(of reporting period)*	Reporting Period 01.01.2025 to 30.09.2025		Country/Continent (No of Countries) *(since beginning of routine phase)*	Since beginning of routine phase until 30.09.2025 (end of reporting period)
European	Europe *(23)*	132		Europe *(36)*	2450
European Countries	• Germany	48		• Germany	962
	• Italy	11		• Italy	228
	• United Kingdom	11		• France	218
	• Spain	10		• United Kingdom	157
	• Netherlands	9		• Spain	145
	• France	6		• Netherlands	116
	• Austria	5		• Poland	104
	• Romania	5		• Finland	52
	• Greece	4		• Belgium	48
	• Ireland	4		• Greece	46
	• Switzerland	4		• Switzerland	42
	• Poland	3		• Austria	40
	• Belgium	2		• Portugal	38
	• Czechia	1		• Sweden	37
	• Denmark	1		• Norway	36
	• Estonia	1		• Czechia	33
	• Others *(7)*	0		• Others *(19)*	148
Non European	North America *(5)*	46		North America *(16)*	733
	South America *(8)*	47		South America *(10)*	342
	Asia *(24)*	261		Asia *(34)*	1707
	Africa *(17)*	38		Africa *(37)*	290
	Oceania *(2)*	19		Oceania *(3)*	224
	Total *(79)*	**543**		**Total *(130)***	**5746**

Table 5-1 Number of registered users per continent (number of user countries during reporting period)

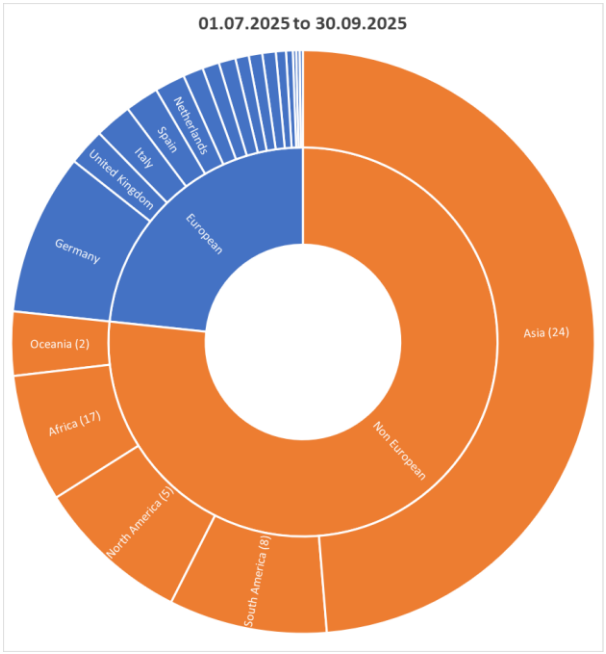

Reporting Period 01.07.2025 to 30.09.2025 with a total of 543 Users of 79 different countries.

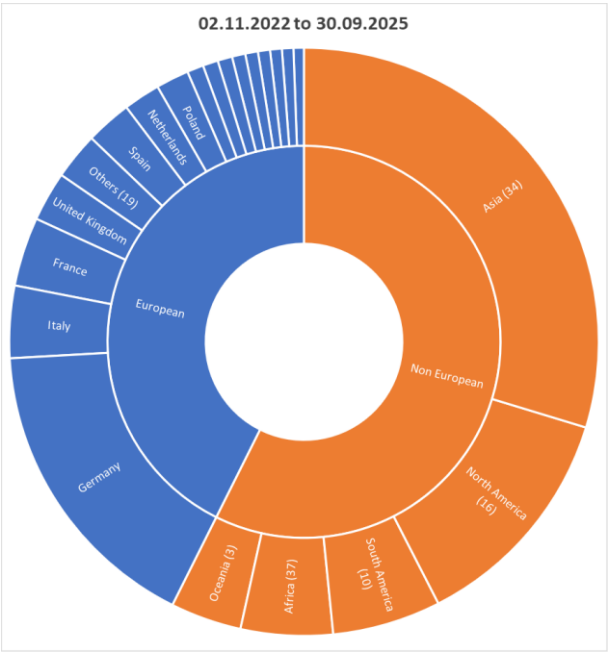

Since beginning of operational phase until 30.09.2025 (end of reporting period) with total of 5746 Users of 130 different countries.

Figure 5-1 Number of registered users per country

User per Category		New within reporting period 01.07.2025 to 30.09.2025	Since beginning of routine phase start until 30.09.2025 (end of reporting period)
Registered users	Total*	543	5746
	with active role assignment**	443	4407
Cat-1 Science	Total	365	4389
	AO Process 00001**	365	3522
	AO Process 00002**	0	641
	AO Process 00003**	0	225
Cat-2 Commercial	Total	11	42
Cat-1 Distributor***	Total	293	3339

Table 5-2 Number of registered users and number of released user roles per category (Cat-1 Science, Cat-2 Commercial and Cat-1 Distributor)

* Registered users inhibited user accounts excluded

**Registered users with at least one active user role

***Catalogue User, ordering EnMAP data from archive

Notice that registered users belong to different categories, therefore the sum of Cat-1 Science and Cat-1 Distributors or other categories does not correspond to the total registered users.

5.2 Announcements-of-Opportunities

Announcement -of-Opportunity	New within reporting period 01.07.2025 to 30.09.2025		Since beginning of routine Phase until 30.09.2025 (end of reporting period)	
	Proposals	Total tiles granted	Proposals	Total tiles granted
A00001	81	4317	849	37236
A00002	0	0	126	10395
A00003	0	0	4	127
Total	81	4317	979	47758

Table 5-3 Number of released science proposals per Announcement-of-Opportunity (AOs#) and total number of granted tiles per AO#.

Icon	Topic	New within reporting period 01.07.2025 to 30.09.2025		Since beginning of routine Phase until 30.09.2025 (end of reporting period)	
		Proposal	Total tiles granted	Proposal	Total tiles granted
	ATMOSPHERE	3	291	53	3289
	CAL/VAL	1	105	39	5330
	GEO/SOIL	35	1308	322	9856
	HAZARD/RISK	2	30	23	722
	METHODS	2	99	21	812
	SNOW/ICE	3	366	24	1547
	URBAN	2	117	15	593
	VEGETATION	27	1671	370	20591
	WATER	6	330	112	5018
	Total	**81**	**4317**	**979**	**47758**

Table 5-4 Number of accepted science proposals and total number of granted tiles per topic

6 Archived and Delivered Observations

The following table shows the number of archived Earth Observation and Calibration products and their sizes within the specified time frames.

Acquisition Type	Archived	Reporting Period 01.07.2025 to 30.09.2025		Since beginning of Commissioning Phase until 30.09.2025 (end of reporting period)	
		Number Tiles / Observations	Size (in GB)	Number Tiles / Observations	Size (in GB)
Earth Observation (EO)	Total	20625 / 2176	10049.90	214711 / 19765	104621.79
	Average / Day	224.18 / 23.65	109.23	167.87 / 15.45	81.79
Calibration (CAL)	Total	27	112.74	465	1941.71
	Average / Day	0.29	1.22	0.36	1.51

Table 6-1 Number and size of archived and not archived products (more than one version of the same image can be archived)

The following table shows the number of delivered products and their sizes within the specified time frames. Product deliveries result either directly from acquisition orders (“Acquisition”) or catalog orders (“Archive”).

Acquisition Type	Order Type		Reporting Period 01.07.2025 to 30.09.2025		Since beginning of Commissioning Phase until 30.09.2025 (end of reporting period)	
			Number Tiles / Observations	Size (in GB)	Number Tiles / Observations	Size (in GB)
Earth Observation (EO)	Acquisition	Total	22117 / 2219	9724.60	180351 / 16722	79850.63
		Average / Day	240.40 / 24.11	105.70	141.00 / 13.07	62.43
	Catalogue	Total	14256	5067.19	142062	53229.64
		Average / Day	154.95	55.07	111.07	41.61
Calibration (CAL)	Acquisition	Total	27	111.61	297	1261.94
		Average / Day	0.29	1.21	0.23	0.98
	Catalogue	Total	0	0.0	77	394.93
		Average / Day	0.0	0.0	0.06	0.30

Table 6-2 Number and size of delivered products

6.1 Archived Acquisitions

The following figures show the heatmaps for the whole world and for Europe within the specified time frames. The heatmaps represent the frequencies of products at a geographic location, where the number of products increases from blue over red to yellow.

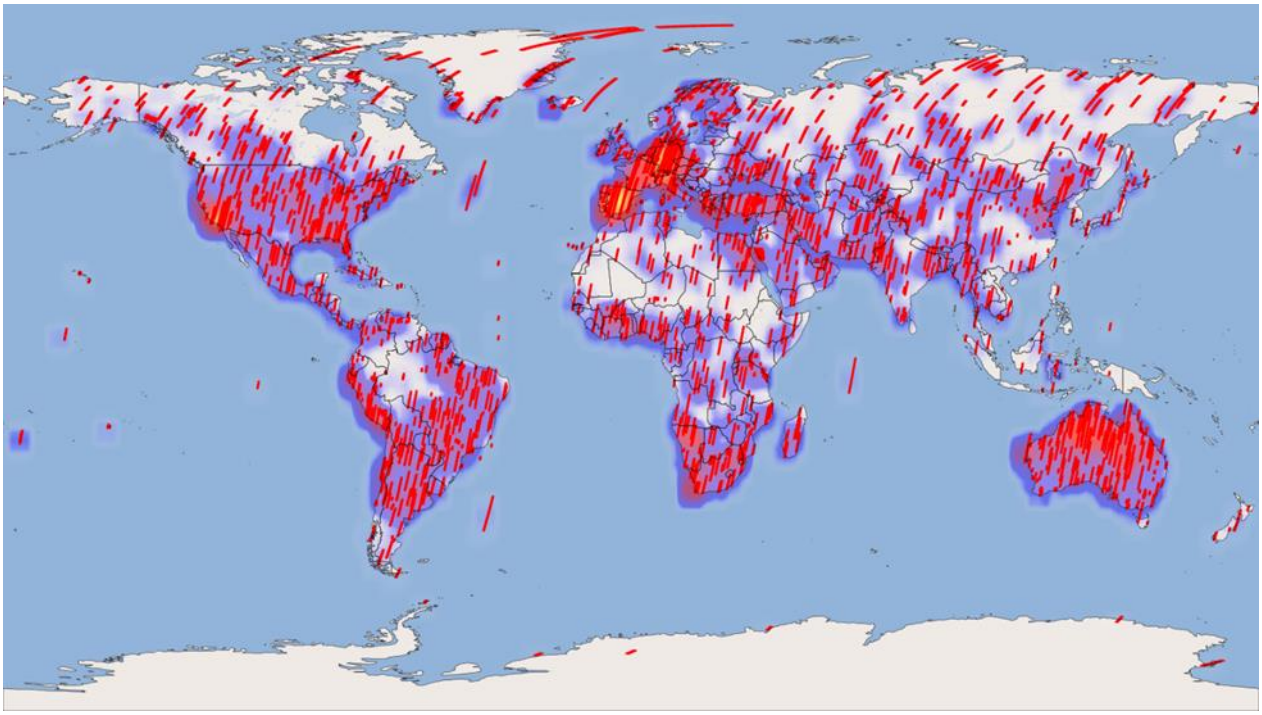

reporting period 01.07.2025 to 30.09.2025

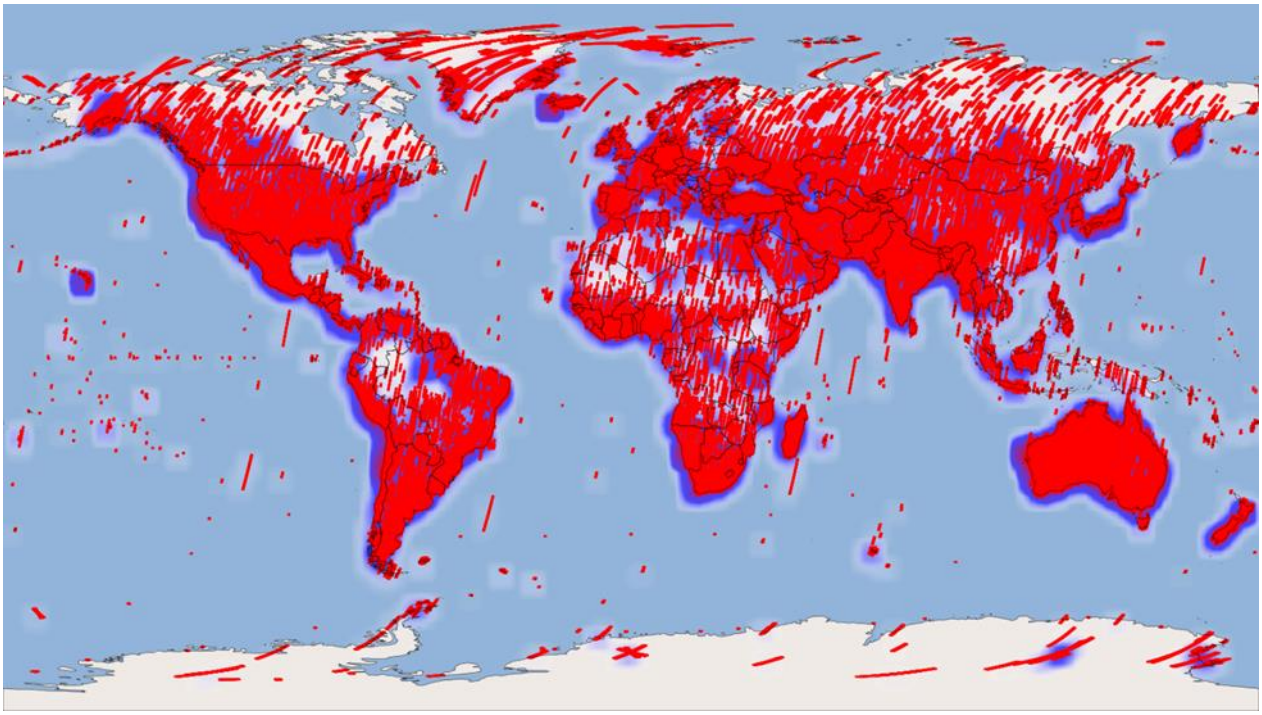

reporting period 2022-04-01 to 30.09.2025 includes commissioning phase acquisitions and different versions of the same tiles)

Figure 6-1 Geographic location of all Earth observation tiles archived, World

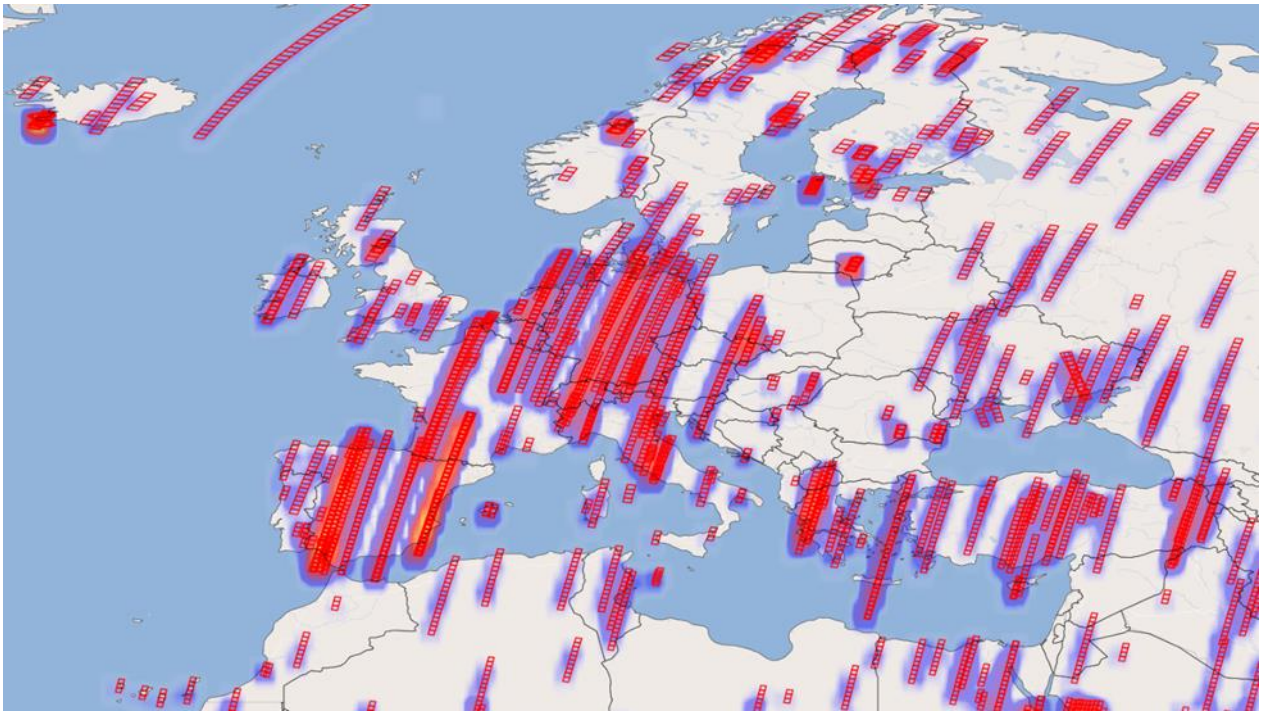

reporting period 01.07.2025 to 30.09.2025 Europe

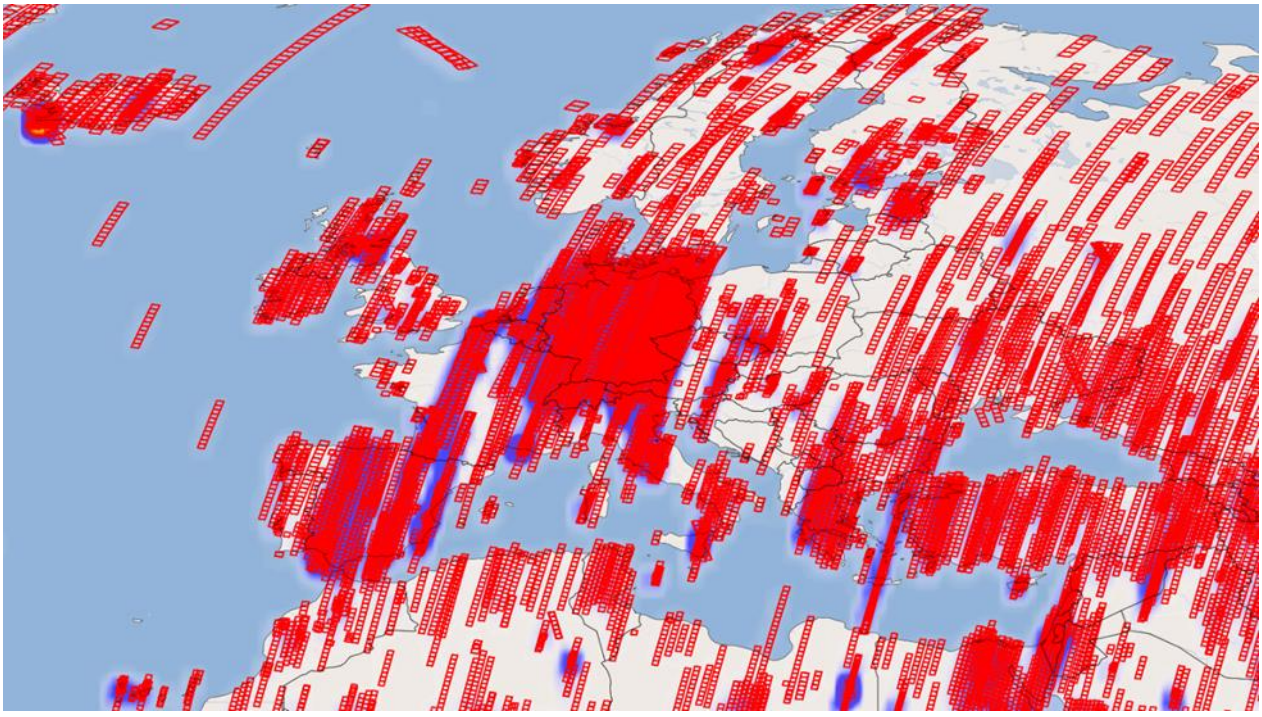

reporting period 2022-04-01 to 30.09.2025 Europe (includes commissioning phase acquisitions)

Figure 6-2 Geographic location of all Earth observation tiles archived, Europe

The following figures show the distribution of cloud coverage for the archived products.

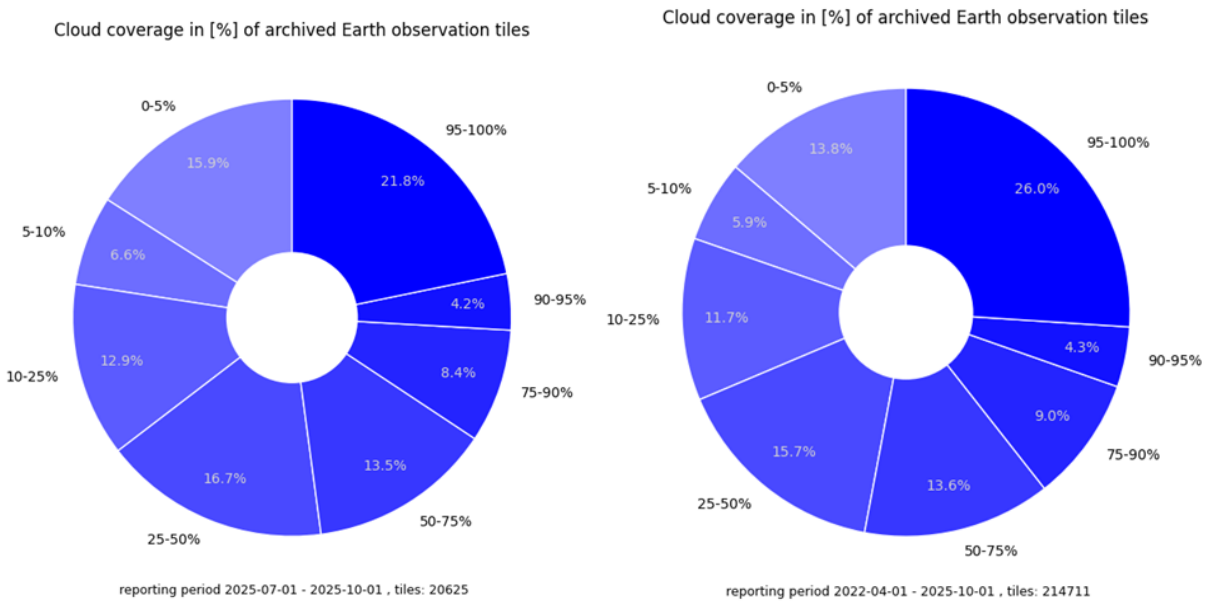

Figure 6-3 Cloud coverage in [%] of archived Earth observation tiles

The following figures show the distribution of observation angles for the archived products.

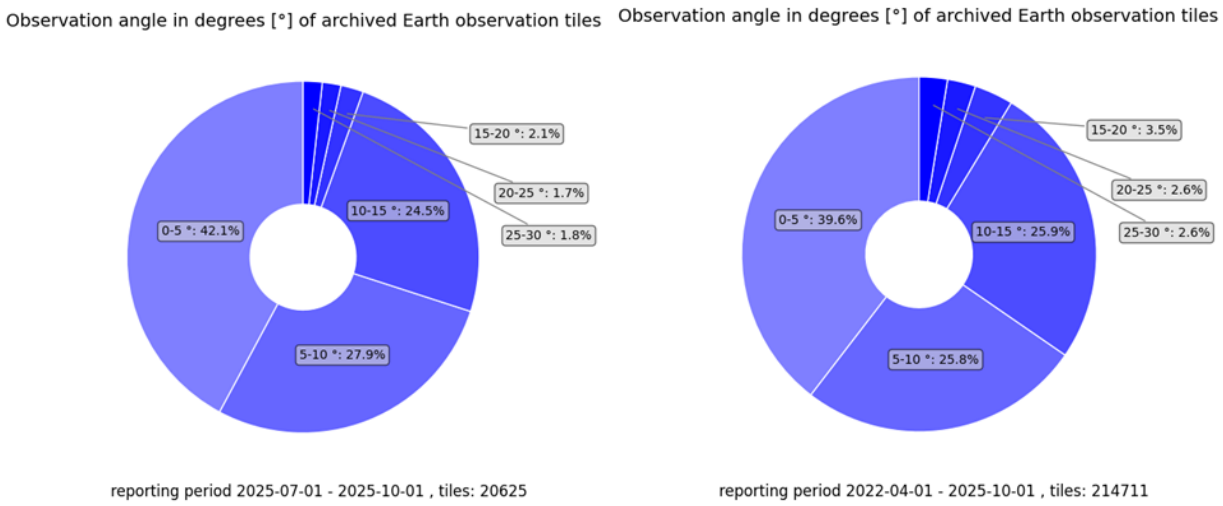

Figure 6-4 Observation angle of archived Earth observation tiles

6.2 Delivered Observations

The following figures show the distribution of processing level of the delivered products from acquisition orders.

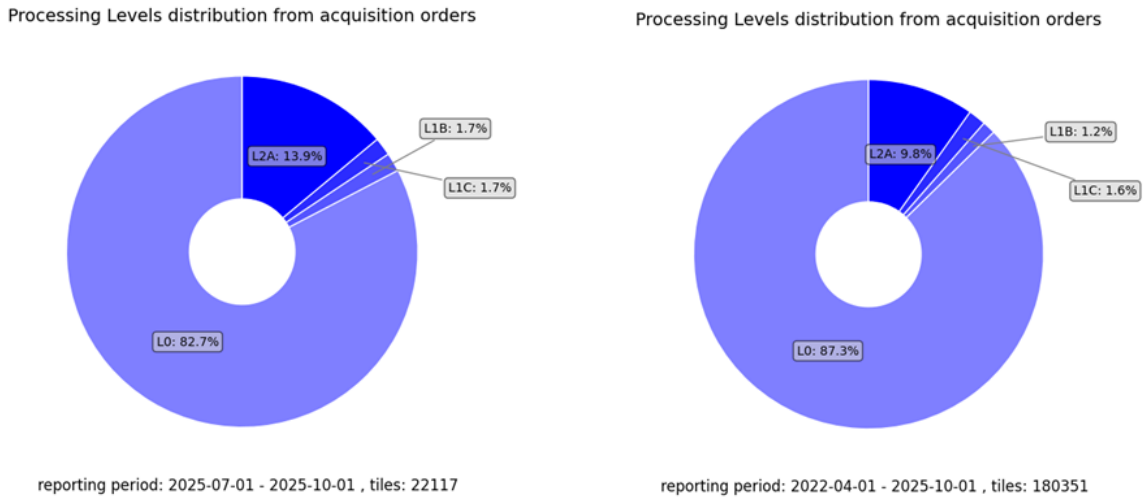

Figure 6-5 Levels of delivered Earth observation tiles from acquisition orders

The following figures show the distribution of processing level and correction type (for L2A) of the delivered products from catalog orders.

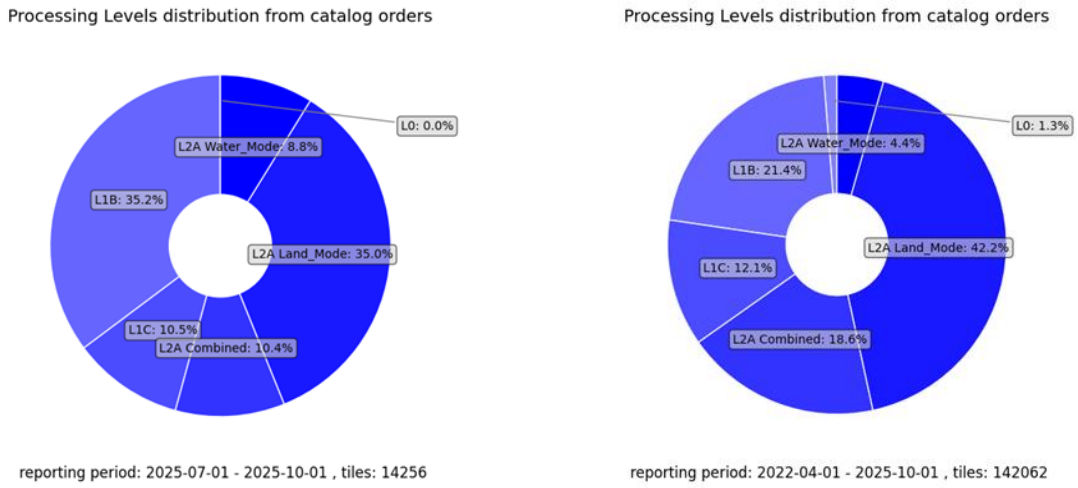

Figure 6-6 Levels of delivered Earth observation tiles from catalog orders

6.2.1 Delivered L2A products from the Download service (EOC Geoservice)

The Ground Segment also produces products already processed with standard parameters. CEOS certified L2A ARD products are available for direct download using the EOC Geoservice and the EOLab platforms. Since July 2025, the IPP account credentials also grant access to the EOC Geoservice to download EnMAP products.

EnMAP's Ground Segment processes all recorded data to L2A ARD format, saving computational and processing time. The default processing parameters of the L2A ARD are the following:

Product_Format = **GeoTIFF+Metadata**
Map Projection = **UTM_Zone_of_Scene_Center**
Image Resampling = **Bilinear_Interpolation**
Correction Type = **Land_Mode**
Cirrus Haze Removal = **No**
Band Interpolation = **No**
Terrain Correction = **Automatic**
Season = **Automatic**
Ozone column = **Automatic**

Table 6-3 Processing parameters used for the L2A ARD products in Geoservice / EOLab

In addition, take into account that:

- the versions of the L2A ARD products may differ depending on their generation time. The processor changelog (https://www.enmap.org/data/doc/EnMAP_processor_changelog.pdf) provides an overview of the software changes. During re-processing of the L2A ARD products, new versions of the products will replace older versions of the products. Currently a re-processing is in progress that shall bring all L2A products to at least version **V01.05.02**.

- No L2A-water products are available as L2A ARD products in Geoservice. For the moment water processing is only available using the on-demand processing options in EOWeb.

- The L2A ARD archive is now complete. All EnMAP products available in the Mission archive are also available as L2A ARD products at Geoservice / EOLab.

The total number of downloads using the EOC Geoservice is **986979** for this reporting period (01.07.2025 to 30.09.2025). Number of monthly downloads for this quarter are given in Table 6-4 and the graph with their evolution since the start of the service is shown in Figure 6-7.

Product	Month	# Downloads
ENMAP-L2A	2025-07	66474
ENMAP-L2A	2025-08	324729
ENMAP-L2A	2025-09	595776
Total in period		986979

Table 6-4 Absolut amount of downloads in Geoservice

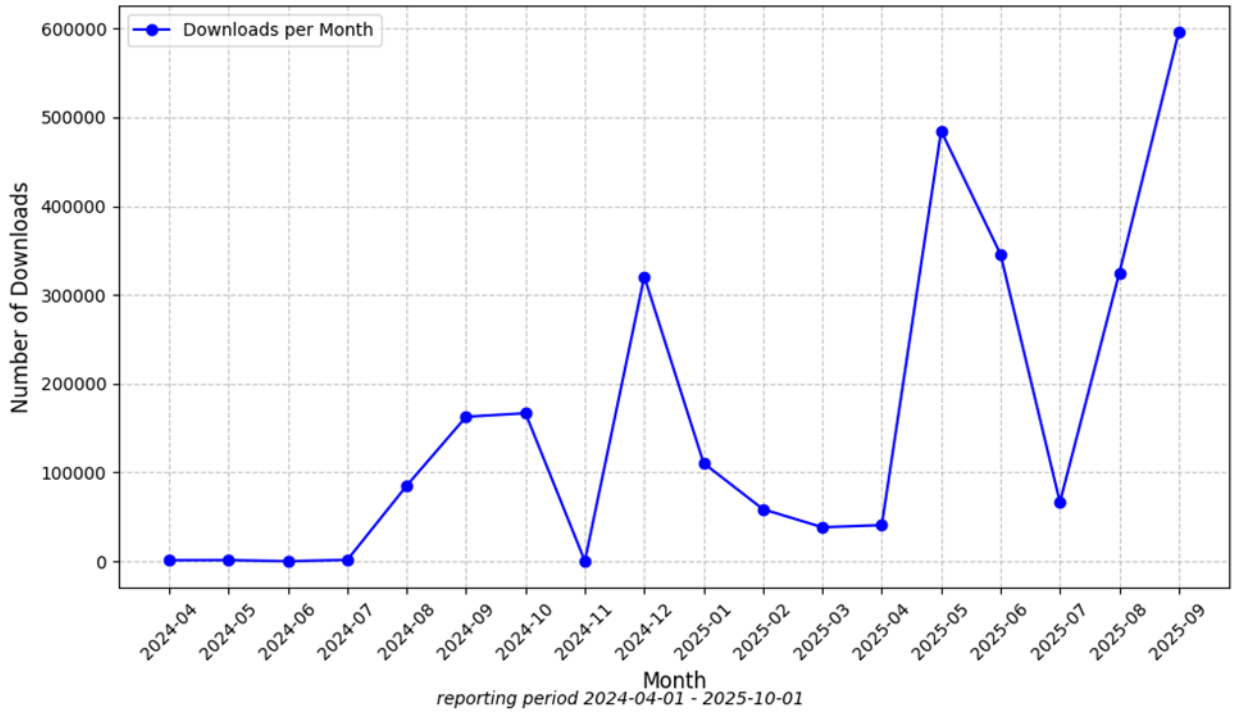

Figure 6-7 Downloads in Geoservice per month

7 Detailed Status

7.1 Satellite

During the reporting period the mission has experienced 1 HSI SAFE_ERROR events that have resulted in the loss of observation time. The event took place on 07.08.2025 but only resulted in a few hours of outage since the operations could be resumed next day, on 08.08.2025. In addition, a DSHA Safety Mode event took place on 29.09.2025 and was recovered next day by the operations team. As reported in all the previous events of these typee, no consequences on the image or data quality are observed as a result of these events. For more details on data quality see sections 7.6 and 8.

The sporadic cancellation of acquisitions when the satellite is coming from the eclipse phase (known as “3-minute events”), has not been observed during most of the period, but towards the end of August it started to appear again like it was observed in previous years.

More details about different satellite aspects are reported in the following subsections.

7.1.1 Orbit

The reference orbit is a Sun-synchronous polar orbit with a mean local time of descending node of 11:00 hrs and a repeat cycle of 398 revolutions in 27 days at an altitude of 643 km.

The satellite orbit is controlled with respect to an Earth-fixed reference track over the entire orbit, analogous to a rim, with a control box of +/- 6 km in radial direction and +/- 22 km in normal direction.

During Q3 2025, a total of 1824 ACS Precise Modes were executed onBoard, compared to 1780 during the previous quarter. Due to the implementation of Back-to-Back Image Acquisitions, the number of ACS Precise Modes does not represent the number of performed activities. By executing two or three Images as one sequence, the total number of ACS Precise Modes decreases whereas the number of Image Acquisitions remains stable or increases. Over the whole mission, a total of 21358 ACS Precise Modes have been successfully executed.

During Q3 2025, two in-plane and two out-of-plane maneuvers were executed. No collision avoidance maneuvers were required. The resulting performance error off all maneuvers was estimated by FDS to be between -0.9% and -0.3%. No actuations of the Ball Latch Valve or other OCS configuration changes were performed during Q3 2025**.**

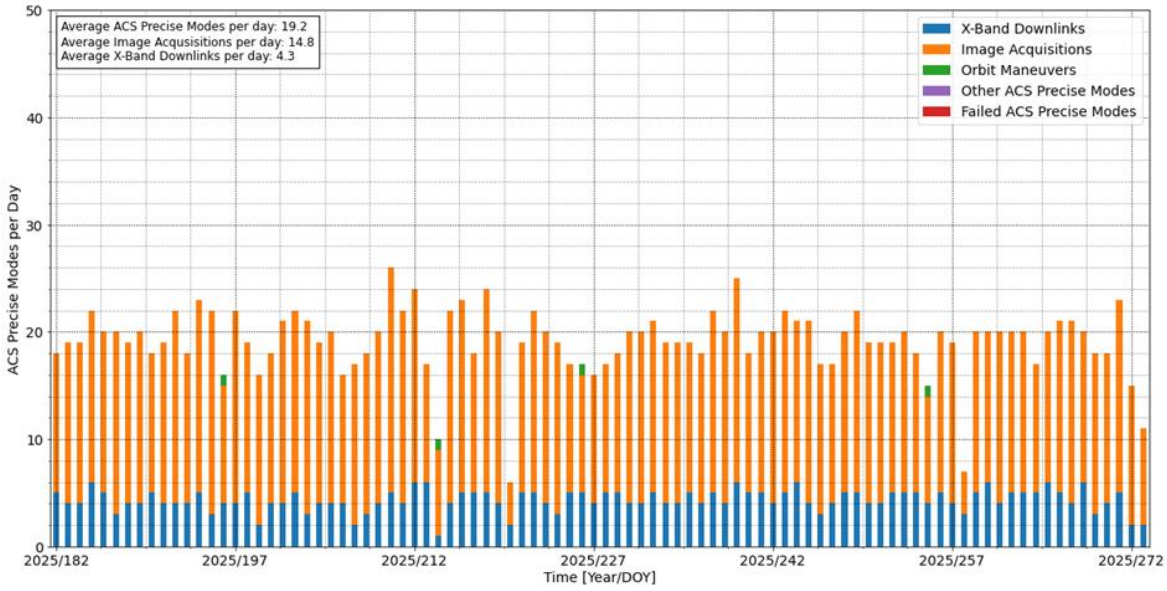

Figure 7-1 Number of ACS Precise Modes per day during Q3 2025

7.1.2 Life Limited Items

The life cycle of the life limited items is evaluated depending on their use. The life-limited items include the following optical and mechanical components:

Life-Limited Item	01.07.2025 to 30.09.2025	until 30.09.2025	Estimated minimum total lifetime / health of the system
Fuel(*)	+0.4 kg	8.8 kg	17.0 years
Battery and Solar Cells(**)	nominal	nominal	Nominal
Shutter Usage	+2.52%	23.09%	15.2 years (@ daily use)
FAD movements	+1.00%	30%	15.2 years (@ bimonthly use)
Diffuser exposure time based on sole measurement time(***)	+1.67%	50.00%	8.5 years (@ bimonthly use to reach 100% originally planned used)
Diffuser exposure time based on real cyclogram duration(***)	+2.00%	59.90%	6.8 years (@ bimonthly use to reach 100% originally planned used)
On-Board Calibration Equipment Usage	On-board calibration equipment:		
- OBCA SPC lamp 1	+1.41%	16.86%	19.4 years (@ biweekly use)
- OBCA RAD lamp 1/LED 1	+3.39%	35.22%	8.3 years (@ weekly use)
- FPA LEDs 1	+0.56%	7.86%	44.5 years (@ monthly use)

Table 7-1 Status of life-limited items

(*) During periods with higher temperature and pressure fluctuations due to e.g., an Instrument shutdown and startup, the calculation of the propellant mass via the Pressure-Volume-Temperature method contains a relatively large margin of errors.

(**) The Power Subsystem is working nominally and as expected. Voltage stays above any critical level.

(***) A 100% Sun diffuser exposure time corresponds to a total planned exposure of 2 hours after 5 years when performing monthly Solar calibrations. The contribution of the diffuser to the total radiometric uncertainty after reaching the reference 100% value is estimated to be **0.6%** according to the instrument manufacturer. This value is significantly below the 5% total radiometric uncertainty requirement, which indicates that the diffuser will not be a relevant contributor to the total radiometric uncertainty of the instrument even if the diffuser were to be used significantly above the originally allocated 2 hours of exposure time (reference 100% value). Nevertheless, the use of the diffuser is continuously monitored and accounted for in the Life-Limited Item list and thanks to the instrument stability the Sun calibration frequency is adjusted to reduce the number of necessary Solar calibrations.

The consumed resources (except fuel) are calculated based on the processed L0 product metadata, i.e. only successfully processed calibrations can be considered.

7.1.3 Redundancies

To date, the SWIR wavelength range is covered by SWIR-A (SWIR-B can be activated using a one-time switch mechanism).

All satellite subsystems are using nominal configurations.

7.2 Ground Stations

7.2.1 S-Band

S-Band Ground Stations	01.07.2025 to 30.09.2025		
	Total Passes	Non-Routine Passes (e.g. Anomaly Handling/SW Updates)	Failed Passes
All stations (Weilheim-Germany, Neustrelitz-Germany, Inuvik-Canada, O'Higgins-Antarctica, Svalbard-Norway)	554 (193 WHM, 214 NSG, 147 INU)	0	2

Table 7-2 S-Band Ground Station Passes

7.2.2 X-Band

X-Band Ground Stations	01.07.2025 to 30.09.2025	
	Executed Passes	Successful Passes
All stations (Neustrelitz-Germany, Inuvik-Canada)	399 (306 NZ, 93 INU)	399 (306 NZ, 93 INU)

Table 7-3 X-Band Ground Station Passes

Inuvik (Canada) station was integrated in Q4 2023 into the regular operations of the EnMAP Ground Segment for X-Band and S-Band downlinks. After integration, more data and more flexibility in S-band and X-band data reception is achieved, especially concerning image acquisitions over Europe.

7.3 User Interfaces

Further improvements to the user interfaces are continuously on-going and will be reported in this section.

During Q3 2025, Cat-2 users now receive a personalized email after successful role granting providing more information about the procedure how to submit proposals for finally tasking orders.

During the reporting period the Ground Segment of EnMAP continues to update the information on future high priority observations of the EnMAP mission (*Foreground Mission*). The tool displaying this information is available at the EnMAP web site under: https://www.enmap.org/data_tools/foreground_mission/

With this tool the users can get informed weeks in advance about future priority observations with EnMAP. Initially, a set of long flight-lines (990km) over Germany and other European countries have been identified together with the user community and will be regularly scheduled. Since July 2024, the Foreground mission has expanded to include additional European regions. The foreground mission continued in Q3 2025 to focus in Germany and Europe, but it is expected that it shifts to southern Europe and the southern hemisphere during winter time.

7.4 Processors

Reference [3] provides the product specification and [4], [5], [6], [7] the algorithm theoretical basis for Level 1B, Level 1C and Level 2A (land / water).

In the reporting period (01.07.2025 to 30.09.2025) there have been no updates in the EnMAP processing chain. The latest version of the EnMAP processing software was still **V01.05.02**. However, at the time of writing this report a new version of the processing software (**V01.05.05**) has been deployed and is used for data processing since **05.11.2025**.

No changes to the changelog document were made during Q3 2025. The document contains the history of EnMAP processor updates and shows the updates performed in the processing software. The document can be downloaded from the EnMAP website:

https://www.enmap.org/data/doc/EnMAP_processor_changelog.pdf

The following changes are expected to be performed in the future quarters:

- New processor version **V01.05.05**:
  - L2A atmospheric correction over water update (water quality rating and height dependency).
  - L2A improvements in regions around cirrus (fix for aura effects).
  - Fixed WV, VIS and SZA criterion for overall atmospheric quality.
  - Fixed adjacency correction around saturated pixels in L2A products.
  - Treat visibility of neighboring tiles consistently in WV regions in L2A products.
  - Adapted path radiance rescaling, including an adjacency correction, in L2A products.
- Update of the linearity calibration to improve the matching between VNIR and SWIR spectrometers, specially at low radiance level.

7.5 Calibrations

Table 7-4 summarizes the radiometric calibration observations acquired in this quarter and which will be described in the rest of this section. The calibration acquisitions were generally acquired according to the routine operations plan.

Category	01.07.2025 to 30.09.2025	
	Number of Archived Observations	Size (in GB)
Total	27	113.2
Deep Space	3	3.9
Rel. Radiometric	13	50.7
Abs. Radiometric	1	1.3
Linearity	3	51
Spectral Calibration	7	6.3

Table 7-4 Number and size of archived radiometric and spectral calibration observations

The continuous degradation of the VNIR sensor was monitored and quantified. The rate of degradation is constantly decreasing as illustrated in Figure 7-2 and by the end of March 2023 it has reached the point where it is practically negligible and has been kept that way during the reporting period. It shall be noted, though, that this average trend is different at different parts of the detector as illustrated for individual pixels in Figure 7-3. The effect on the radiometric calibration coefficients of a few selected bands is shown in Figure 7-4.

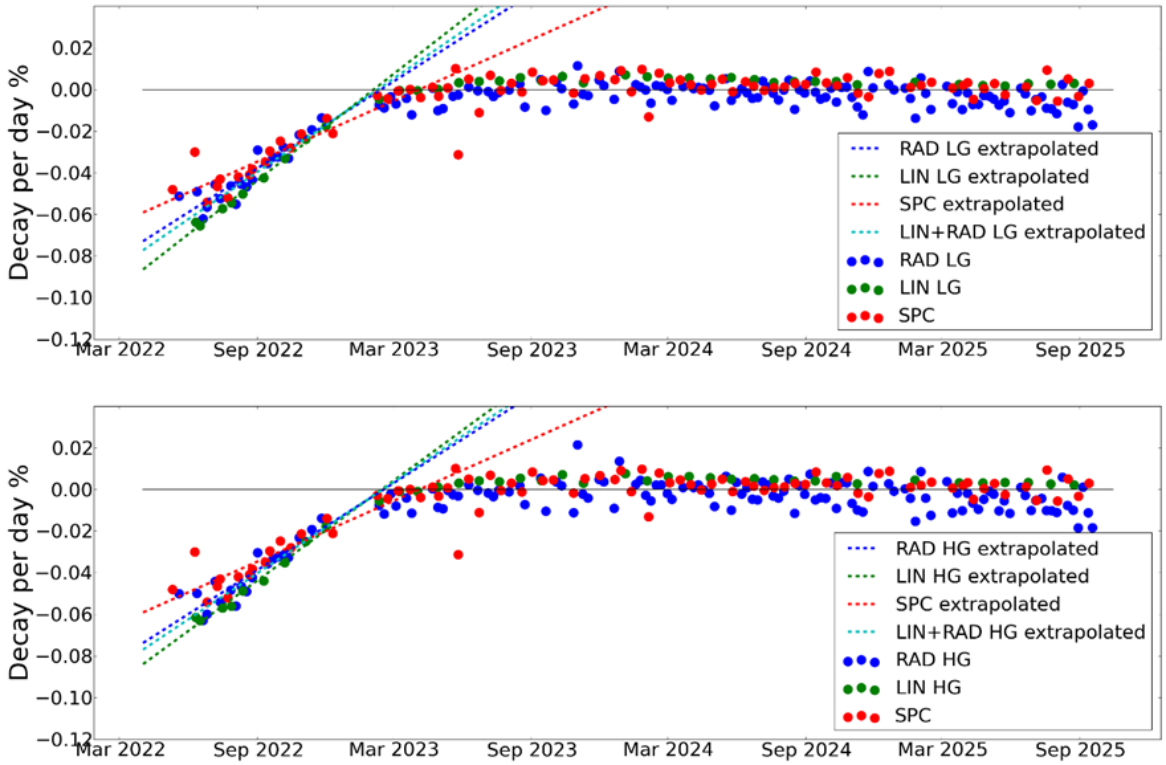

Figure 7-2 Decay per day from Lamp (RAD), Linearity (LIN) and Spectral (SPC) measurements for low gain (top) and high gain (bottom)

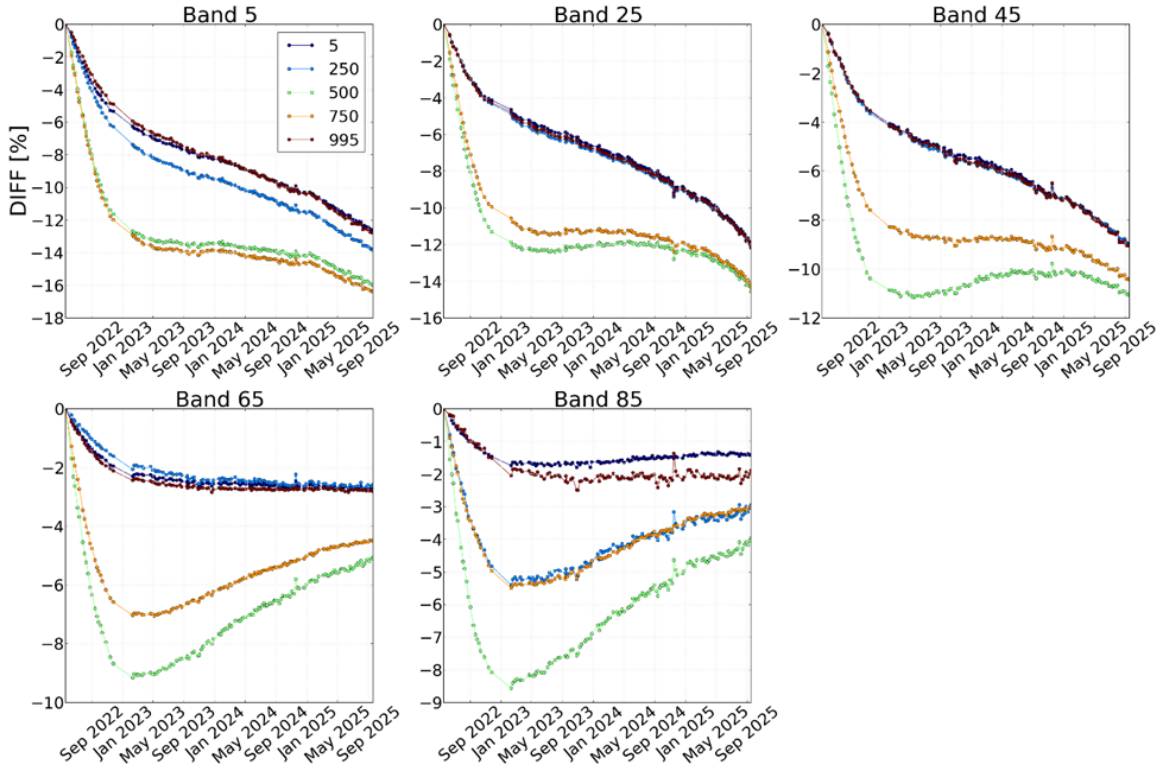

Figure 7-3 Change in percentage for individual pixels based on OBCA-Lamp measurements given for 5 bands and 5 cross track elements (coloured lines).

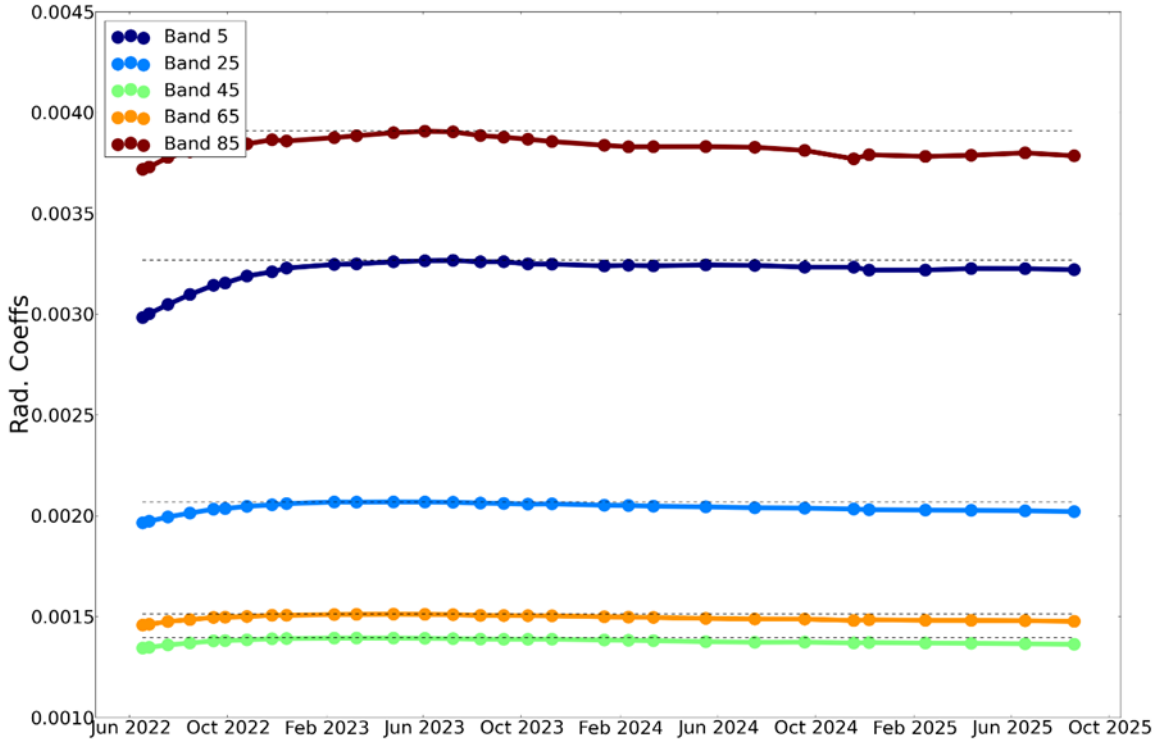

Figure 7-4 Average percentage change in the VNIR radiometric coefficients for five selected bands since launch

7.5.1 Dead Pixels

The following table shows the number and percentage of dead pixels. Figure 7-5 and Figure 7-6 show the position of the dead pixels in the focal plane of VNIR and SWIR sensors respectively. There have been no updates since 31.08.2022.

Defect Pixels	01.07.2025 to 30.09.2025	
	Number of Pixels	Percent
Total	1921	0.8
VNIR	137	0.2
SWIR	1784	1.2

Table 7-5 Number and percent of dead pixels

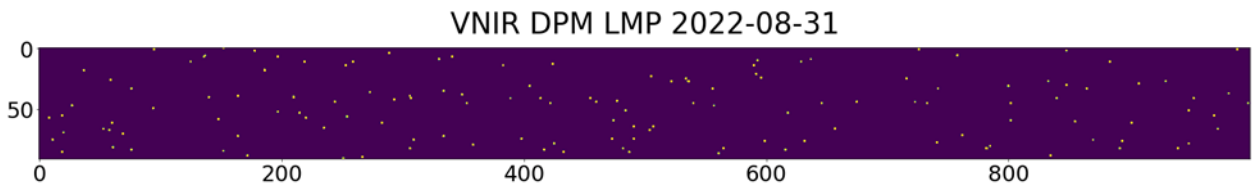

Figure 7-5 VNIR Dead Pixel Mask

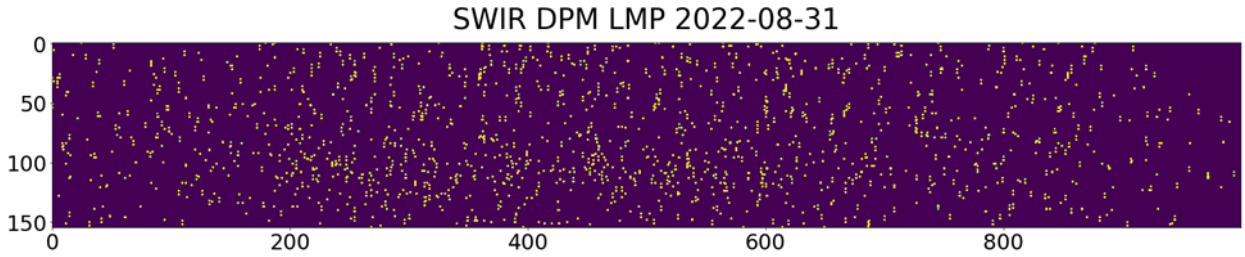

Figure 7-6 SWIR Dead Pixel Mask

There are no clusters of more than three spectrally or spatially adjacent dead pixels.

7.5.2 Spectral Calibration

Remark: In the following figures, OBCA is abbreviation for On-Board Calibration Assembly for spectral and radiometric calibrations.

Category	01.07.2025 to 30.09.2025	
	Number of Archived Observations	Size (in GB)
Total	6	5.4
Spectral Calibration	6	5.4

Table 7-6 Number and size of archived spectral calibration observations

The spectral properties – in particular center wavelength (CW) (see Figure 7-7 and Figure 7-8) and full width at half maximum (FWHM) (see Figure 7-9) for each band (spectral coordinate) and pixel (spatial coordinate) – have been characterized, considering all bands and pixels provided in Level 1B, Level 1C and Level 2A products.

The major conclusions of the monitoring of the spectral performance are summarized as follows:

- During the reporting period, 7 spectral calibration measurements were made which took place on: 04.07.2025, 18.07.2025, 01.08.2025, 15.08.2025, 29.08.2025, 12.09.2025 and 26.09.2025.
- The VNIR spectral range in this reporting period was found to be 418.4 – 993.4 nm over 91 bands (Figure 7-7). The average spectral sampling distance was 6.4 nm with a total range of 4.7 – 8.2 nm. This meets the requirement for overall wavelength coverage [HSI-POSS-0210], average spectral sampling distance [HSI-POSS-0310] and spectral sampling distance range [HSI-POSS-0320].
- The SWIR spectral range in this reporting period was found to be 902.1 – 2445.4 nm over 155 bands (Figure 7-7). The average spectral sampling distance was 10.0 nm with a total range of 7.5 – 12.0 nm. This meets the requirement for overall wavelength coverage [HSI-POSS-0210], average spectral sampling distance [HSI-POSS-0310] and spectral sampling distance range [HSI-POSS-0320].
- The spectral calibration measurements from this quarter show good temporal stability – measurements showed an absolute <0.14 nm change from the VNIR sensor and <0.35 nm change in SWIR (Figure 7-8) with respect to current spectral calibration table. All changes were below 0.5 nm between measurements for VNIR and below 0.5 nm SWIR. This meets the requirement for consecutive spectral stability [HSI-POSS-0510] and overall spectral stability [HSI-POSS-0520].
- FWHM for VNIR and SWIR (Figure 7-9) are shown below but are not recalculated inflight.
- A VNIR degradation pattern is not clearly visible between consecutive spectral reference measurements acquired in this period, but there are positive and negative changes across the detector and on average the signal appears to have increased by 0.05% across all pixels from 20.06.2025 to 26.09.2025. A slightly smaller change was reported in the previous quarter (0.04%). Although small, the monitoring of this behavior will continue in the next reporting period.

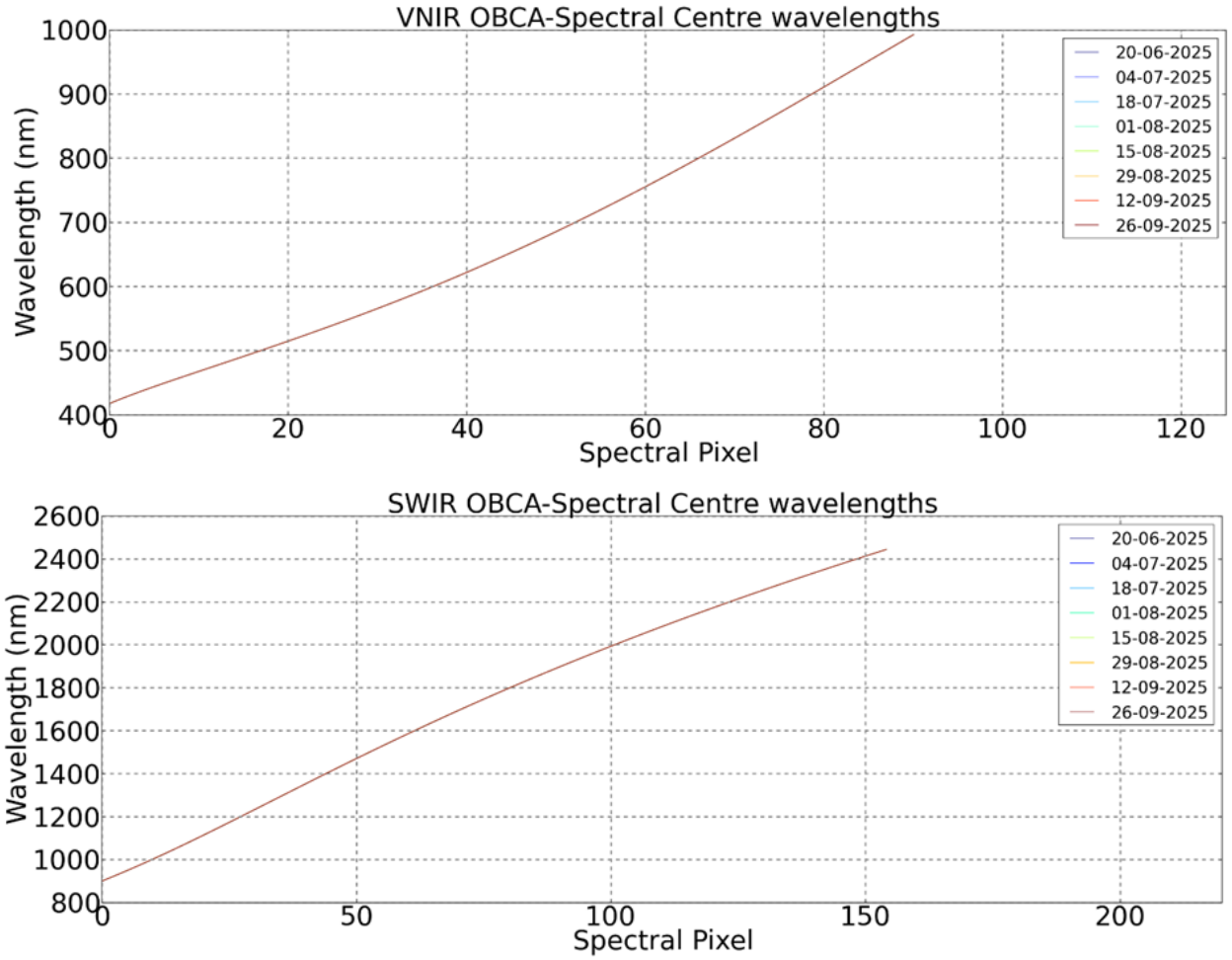

Figure 7-7 VNIR (top) and SWIR (bottom) center wavelength in nm

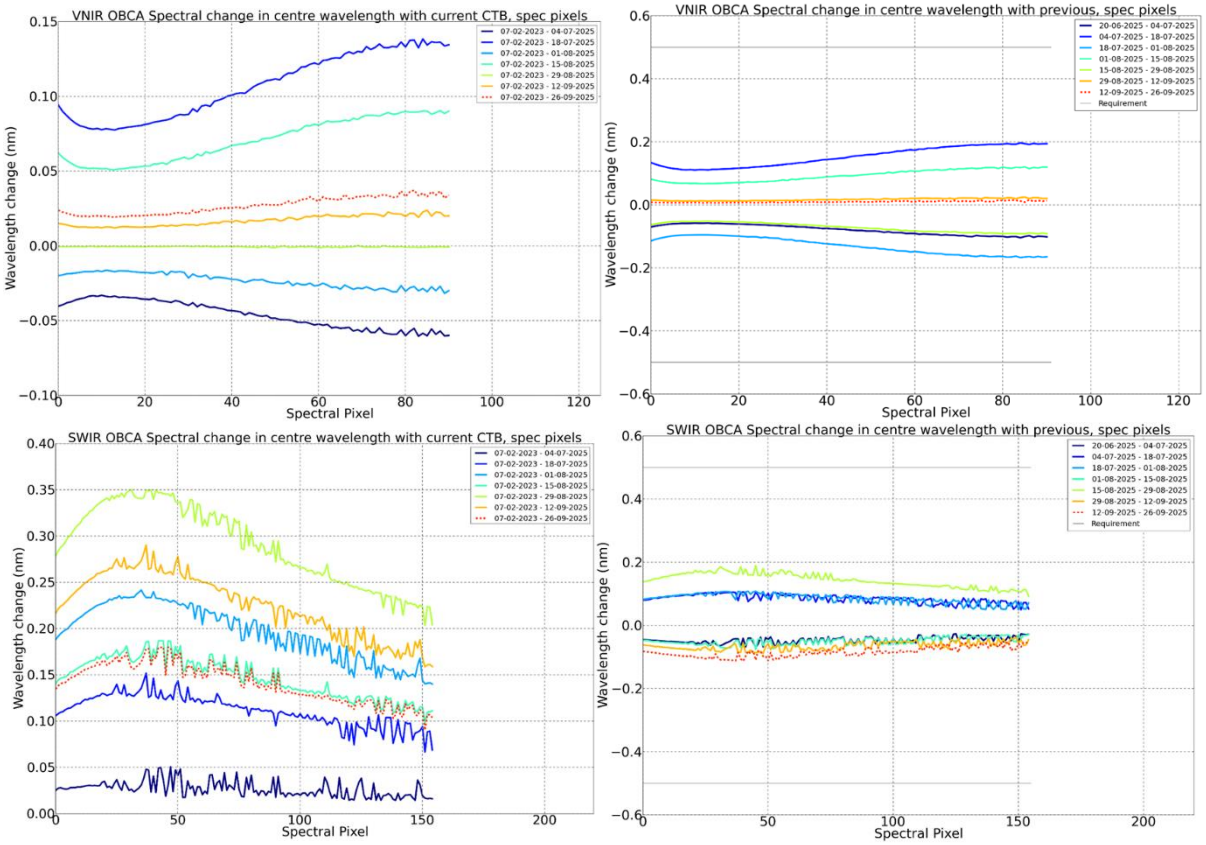

Figure 7-8 Change in center wavelength per spectral pixel for VNIR (top) and SWIR (bottom). Left panels show the changes with respect to current spectral calibration table in use and right panels with respect to the previous measurements.

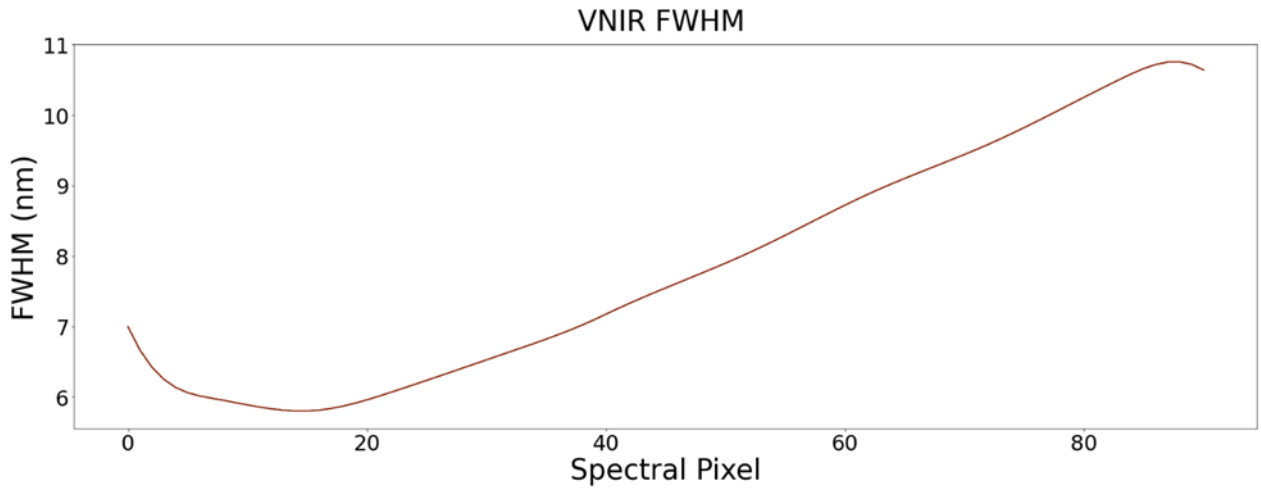

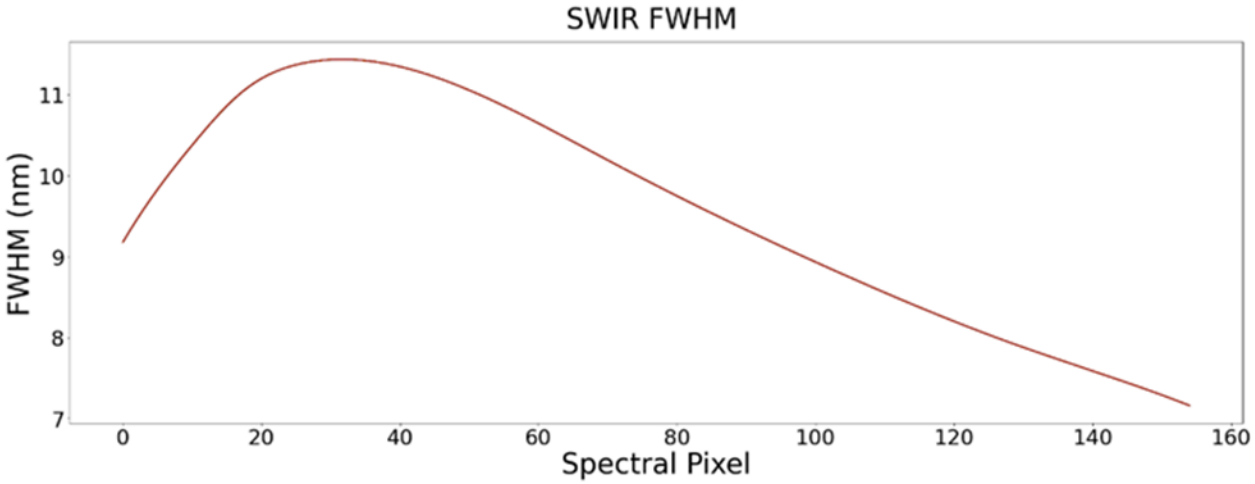

Figure 7-9 VNIR (top) and SWIR (bottom) FWHM in nm

CW and FWHM are available in the spectral calibration tables (see Table 7-7) and System Response Functions (SRF) per band are modelled by a Gaussian shape using those parameters.

Spectral calibration updates

No new calibration products were generated and delivered during the reporting period.

Product	Type	Date of Generation	Date of Validity Start	Date of Validity End	Delivered to

Table 7-7 Generated spectral calibration tables

7.5.3 Radiometric Calibration

Category	01.07.2025 to 30.09.2025	
	Number of Archived Observations	Size (in GB)
Total	20	106.9
Deep Space	3	3.9
Rel. Radiometric	13	50.7
Abs. Radiometric	1	1.3
Linearity	3	51

Table 7-8 Number and size of archived radiometric calibration observations

The radiometric properties – characterized in particular by the calibration coefficient for each band (spectral coordinate) and pixel (spatial coordinate) and radiance – during this reporting period are investigated, considering all bands and pixels and radiances provided in Level 1B, Level 1C and Level 2A products.

Radiometric calibration coefficients (see Figure 7-10, Figure 7-11 and Table 7-10) and VNIR RNU (response non-uniformity, see Figure 7-13) were affected by the degradation of the VNIR sensor during commissioning but have stabilized from Q1 2023. In-flight, the gain matching coefficients (see Figure 7-12), the SWIR calibration coefficients, and the SWIR RNU (response non-uniformity, see Figure 7-13) have been stable.

During the reporting period, one Absolute Radiometric Calibration measurement was obtained. This took place on: 18.08.2025.

Albeit now relatively small in magnitude, changes in the VNIR sensor have led to the creation of new calibration and reference tables for the new absolute radiometric measurement.

Although the VNIR degradation has almost stopped, the overall effects are visible in the reference measurements of the sun. However geometric conditions (sun-earth distance, pointing angle) also play a role in the absolute magnitude so the degradation cannot be quantified with these reference measurements.

The major conclusions of the monitoring of the absolute performance are summarized as follows:

- Changes in the VNIR sensor have affected the absolute Radiometric calibration coefficients: the increasing signal in the VNIR sensor, although not homogeneous, has resulted in decreasing radiometric coefficients. In this reporting period, the calibration coefficients decreased by about -0.2% to offset the increase in absolute (Figure 7-10 and Figure 7-11). Regarding RNU, the degradation features are still visible in the focal plane (Figure 7-13). Lastly, the Gain Matching correction has been relatively stable during this reporting period (Figure 7-12).

- The SWIR sensor has shown good stability during this reporting period, with no significant changes in the gain matching, RNU or radiometric calibration coefficients (Figure 7-10 and Figure 7-11).

- Regarding the total change in calibration corrections as a result of the VNIR degradation, almost all pixels experienced a change of less than 2.5% between consecutive measurements as set in requirement [HSI-POSR-0410]. The only pixels which exceeded this value were already marked as dead during inflight assessment. No SWIR pixels experienced a change of more than 2.5% between consecutive absolute calibration measurements.

- New VNIR and SWIR calibration and reference tables were created for the absolute radiometric measurements from 18.08.2025, mainly due to the changes in the VNIR sensor. The VNIR radiometric calibration coefficients have decreased in this reporting period to offset the increasing VNIR signal. The changes are small, and within requirements, so the dynamic coefficients are not calculated and calibration coefficients are taken directly from the most recent calibration table as envisioned at the beginning of the mission.

- Since April 2024, Absolute Radiometric Calibration measurements are planned at intervals of two months, following the stable performance of both sensors, and to allow for the extension of the lifetime of the solar diffuser.

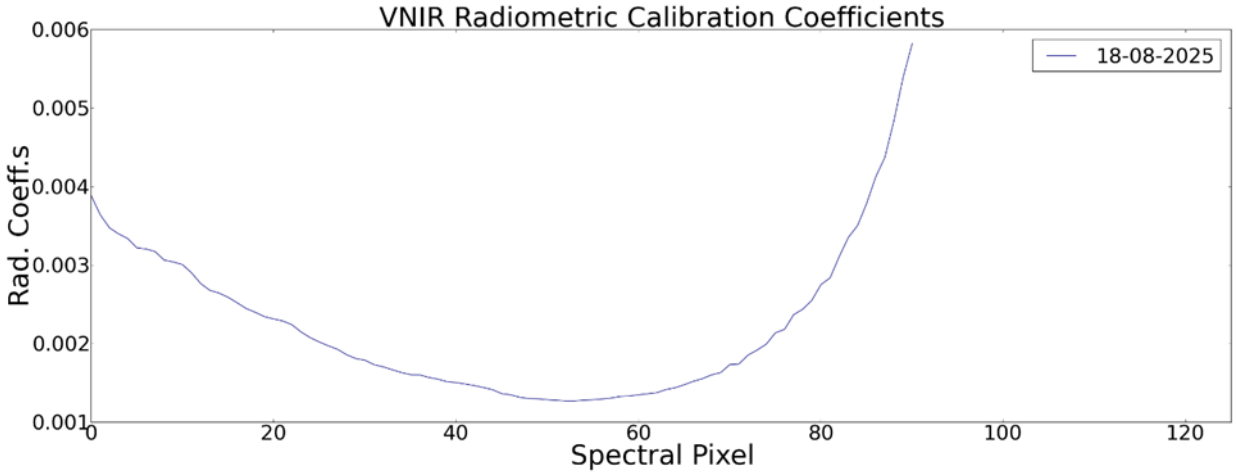

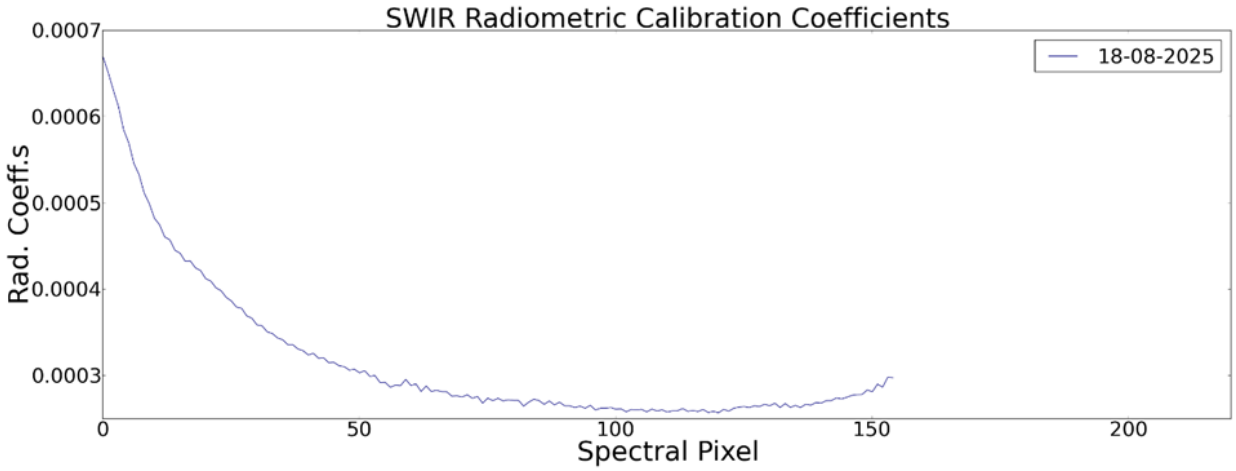

Figure 7-10 VNIR (top) and SWIR (bottom) calibration coefficient in mW/cm²/sr/µm

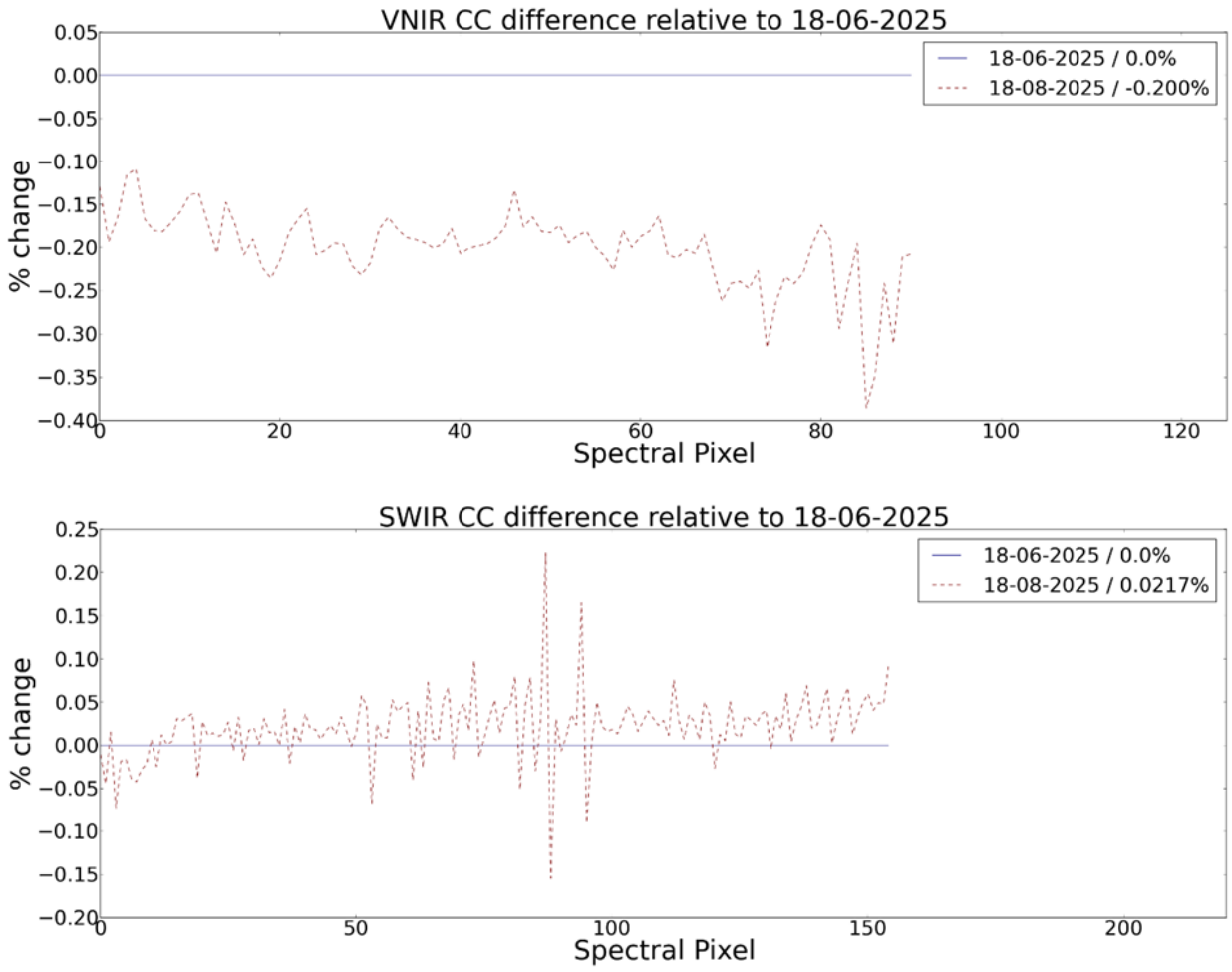

Figure 7-11 Percentage change in VNIR Calibration Coefficients (top) and SWIR Calibration Coefficients (bottom)

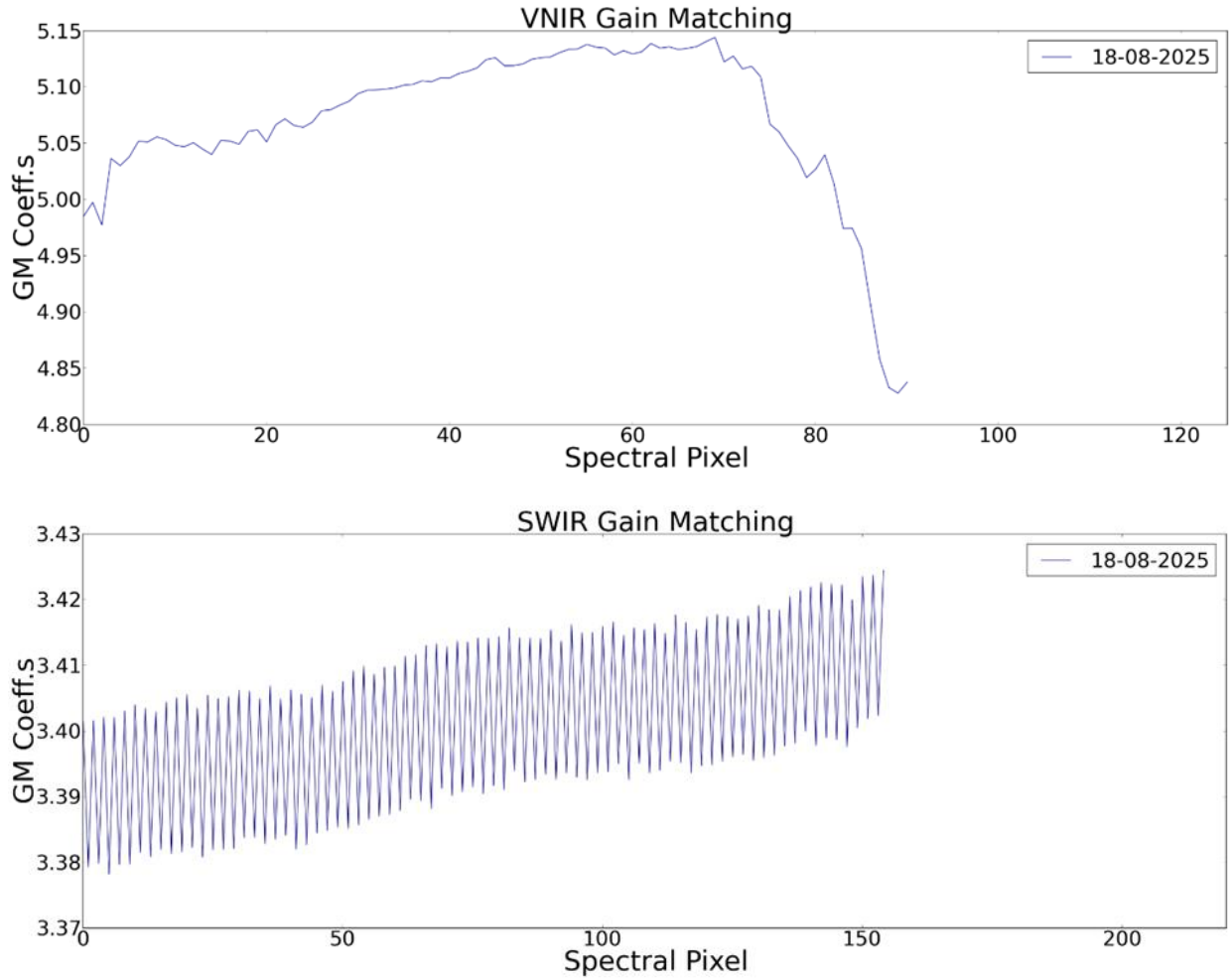

Figure 7-12 VNIR (top) and SWIR (bottom) gain matching calibration coefficients

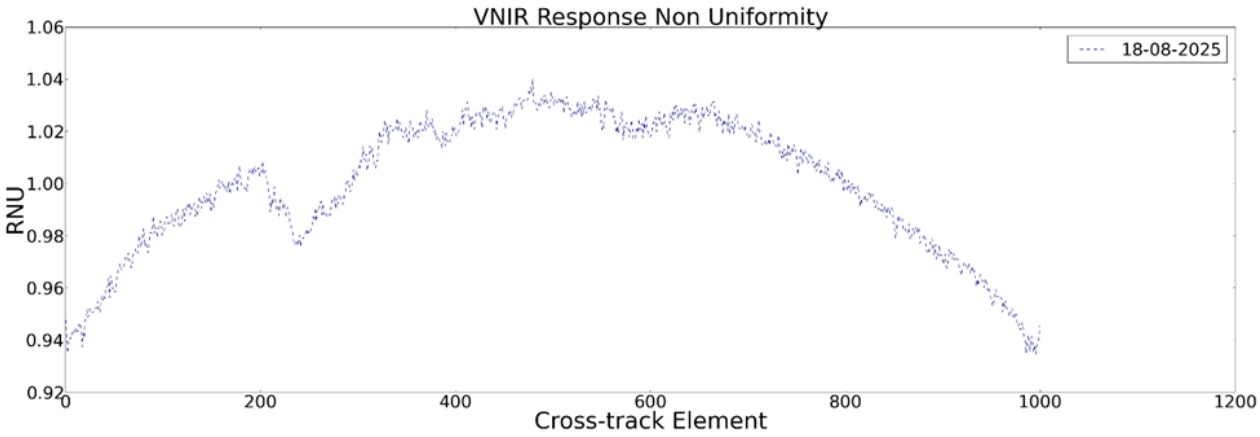

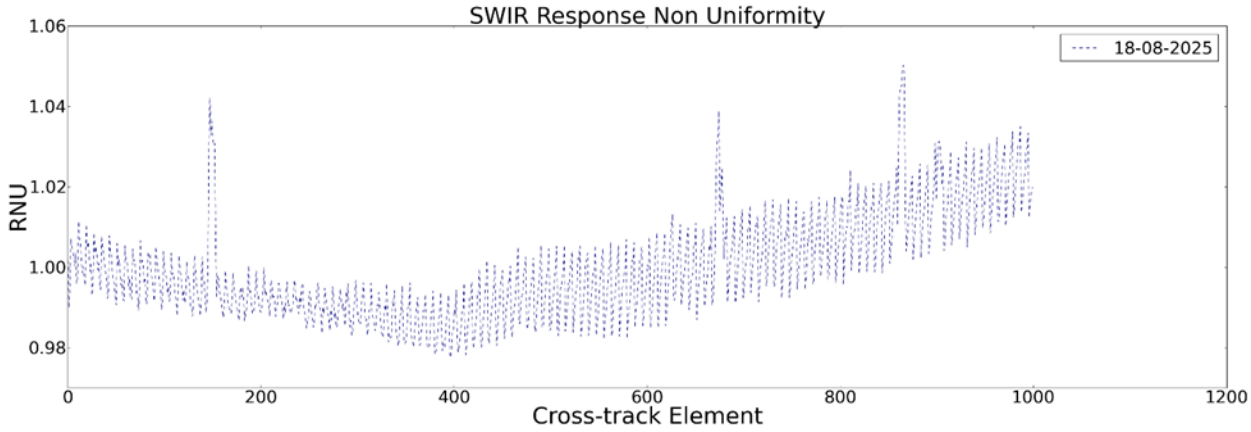

Figure 7-13 VNIR (top) and SWIR (bottom) response non-uniformity coefficients

Signal-to-Noise Ratio

The Signal-to-Noise Ratio (SNR) is derived from the Linearity reference measurements. This is not a perfect set-up for the assessment of the SNR as the linearity measurements only cover a single wavelength and light level at increasing integration times. However, it is well constrained, covering a wide range of radiances including the levels of the reference radiance spectrum that is used to evaluate the requirements (30% reflectance, 30° sun incidence angle, 21 km visibility, target 500 m above sea level). The lamp reference measurements are not used, as the reference spectrum is not well covered at the radiances of the lamp and extrapolation would be required to test the performance at the SNR requirements. Those requirements are: SNR greater than 500 at 495 nm in VNIR for the reference spectrum value given a 10 nm pixel; and SNR greater than 150 at 2200 nm in SWIR for the reference spectrum given a 10 nm pixel.

For the VNIR sensor, SNR is computed from the linearity calibration measurement. SNR values are shown as a contour map with the reference radiance spectrum as a blue line. Contour lines with SNR values of 150 and 500 are also shown in black. The plot in low gain mode includes the mission requirement which is evaluated at 495 nm for a radiance value of 36 mW/cm^2/μm/sr and is expected to be greater than 500: the calculated value here is **596**. The radiance value used here for the evaluation is the value at 495 nm of the reference radiance spectrum after bandwidth normalization to a 10 nm pixel (see Figure 7-15).

For the SWIR sensor, SNR is also computed from the linearity calibration measurement. SNR values for the high gain mode are shown as a contour map with the reference radiance spectrum as a blue line. Contour lines with SNR values of 150 and 500 are also shown in black. The plot in high gain mode includes the mission requirement which is evaluated at 2200 nm for a radiance value of 0.5 mW/cm^2/μm/sr and is expected to be greater than 150: the calculated value here is **201**. The radiance value used here for the evaluation is the value at 2200 nm of the reference radiance spectrum after bandwidth normalization to a 10 nm pixel (see Figure 7-16).

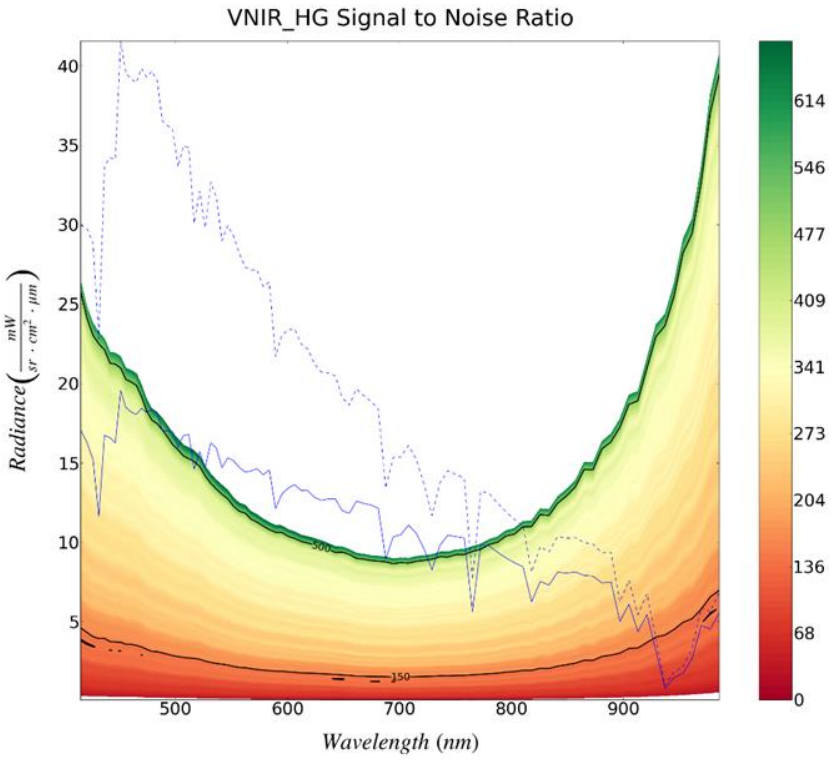

Figure 7-14 SNR contour map for VNIR high gain from the LED linearity observations observed on 17.09.2025. The reference radiance is shown with a blue line and after bandwidth normalization to a 10 nm pixel (dotted). Contour lines with SNR values of 150 and 500 are also shown in black.

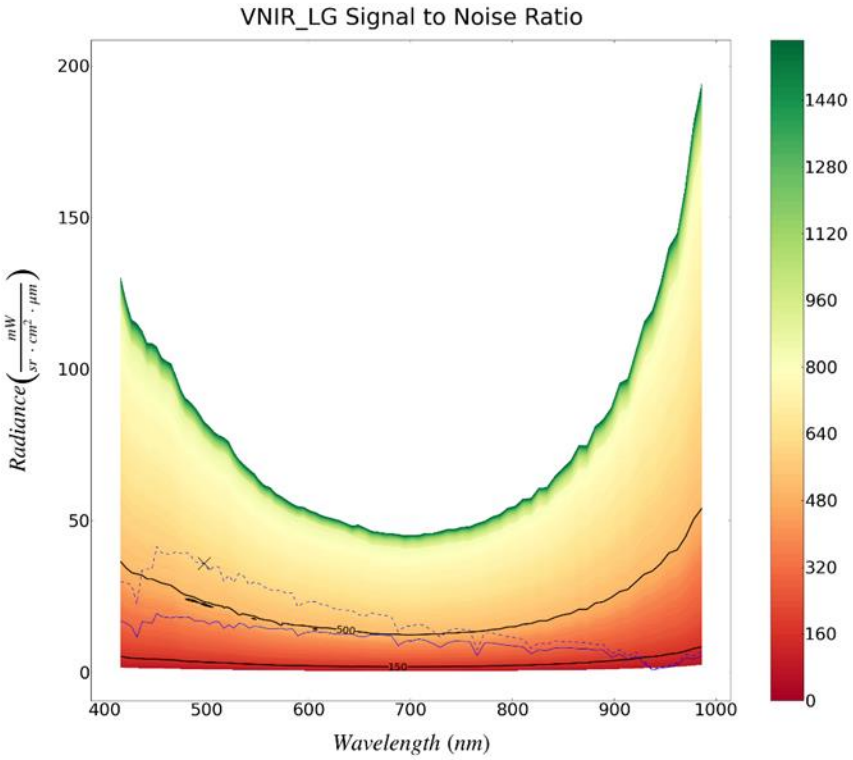

Figure 7-15 SNR contour map for VNIR low gain from the LED linearity observations observed on 17.09.2025. The reference radiance is shown with a blue line and after bandwidth normalization to a 10 nm pixel (dotted). Contour lines with SNR values of 150 and 500 are also shown in black. The mission requirement is evaluated at 495 nm for a radiance value of 36 mW/cm^2/µm/sr (marked with a black cross) and is expected to be greater than 500.

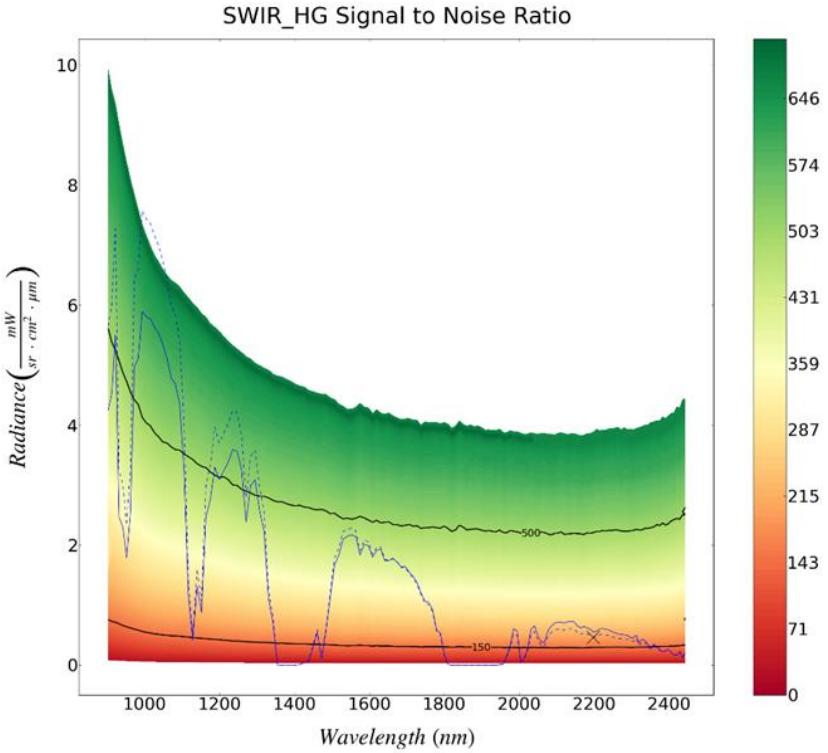

Figure 7-16 SNR contour map for SWIR high gain from the LED linearity observations observed on 17.09.2025. The reference radiance is shown with a blue line and after bandwidth normalization to a 10 nm pixel (dotted). Contour lines with SNR values of 150 and 500 are also shown in black. The mission requirement is evaluated at 2200 nm for a radiance value of 0.5 mW/cm^2/µm/sr (marked with a black cross) and is expected to be greater than 150.

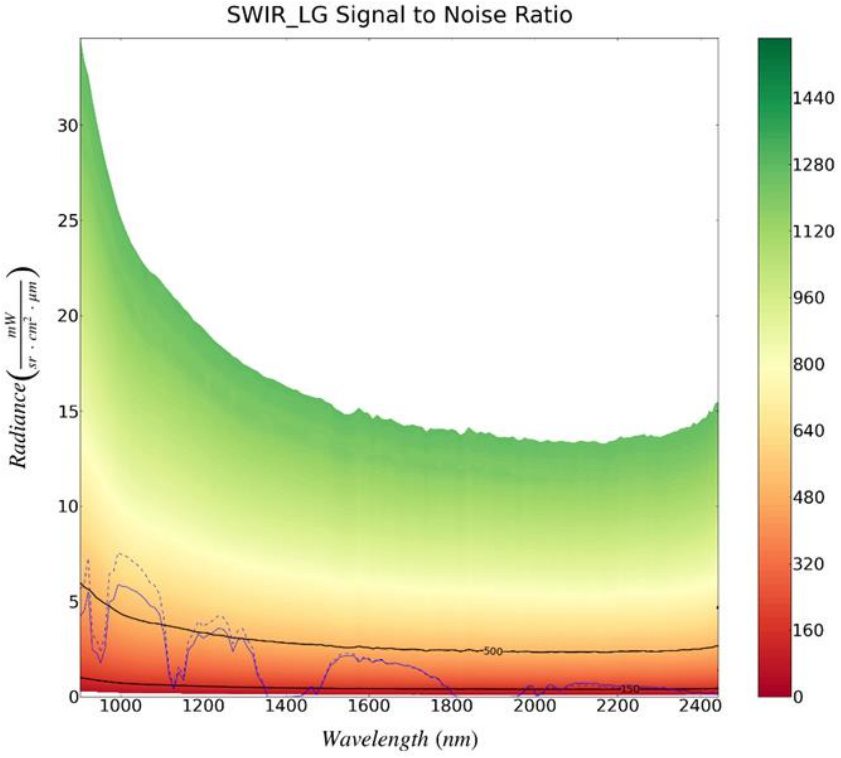

Figure 7-17 SNR contour map for SWIR low gain from the LED linearity observations observed on 17.09.2025. The reference radiance is shown with a blue line and after bandwidth normalization to a 10 nm pixel (dotted). Contour lines with SNR values of 150 and 500 are also shown in black.

The SNR values at the reference radiance spectrum are given in the table below (Table 7-9). The SNR is not determined in absorption regions and when the reference is too low or too high relative to the measured values in the linearity calibration.

Sensor	Wavelength (nm)	Reference Radiance (mW/sr/cm2/µm)	SNR Low gain	SNR High gain
VNIR	415.15	16.70	308.69	318.67
VNIR	420.73	16.30	307.9	316.88
VNIR	426.10	15.23	305.6	310.99
VNIR	431.29	11.66	259.56	276.09
VNIR	436.32	16.76	323.59	337.06
VNIR	441.23	16.62	327.66	334.2
VNIR	446.03	16.28	327.36	339.11
VNIR	450.76	19.57	380.88	373.28
VNIR	455.45	18.50	373.16	375.56
VNIR	460.11	18.24	374.08	376.51
VNIR	464.75	18.08	374.9	377.71
VNIR	469.38	18.46	383.57	397.34
VNIR	474.01	18.20	386.74	479.99
VNIR	478.64	18.40	392.48	
VNIR	483.28	18.18	396.26	
VNIR	487.94	17.08	385.88	
VNIR	492.62	17.03	389.78	
VNIR	497.33	17.01	399.92	
VNIR	502.07	16.01	385.85	
VNIR	506.84	16.75	406.49	
VNIR	511.64	16.82	417.26	
VNIR	516.48	14.64	382.46	
VNIR	521.36	15.74	400.42	
VNIR	526.28	14.73	391.99	
VNIR	531.24	16.29	453.5	
VNIR	536.24	15.97	454.04	
VNIR	541.29	14.72	425.86	
VNIR	546.39	15.34	457.34	
VNIR	551.53	15.17	460.07	
VNIR	556.73	14.75	461.49	
VNIR	561.98	14.44	460.03	
VNIR	567.29	14.51	465.07	
VNIR	572.66	14.67	464.39	
VNIR	578.09	14.27	463.18	
VNIR	583.58	14.59	488.69	
VNIR	589.14	12.15	427.62	
VNIR	594.76	13.06	463.34	
VNIR	600.47	13.44	461.76	
VNIR	606.24	13.65	480.29	
VNIR	612.10	13.29	473.62	
VNIR	618.06	13.28	480.13	
VNIR	624.07	12.84	464.16	
VNIR	630.15	12.66	463.05	
VNIR	636.29	12.75	479.32	
VNIR	642.48	12.76	493.15	
VNIR	648.73	12.02	466.5	
VNIR	655.05	11.85	471.04	
VNIR	661.43	12.62	487.65	
VNIR	667.87	12.47	485.76	
VNIR	674.38	12.37	485.12	
VNIR	680.96	12.17	480.05	
VNIR	687.60	8.98	389.34	
VNIR	694.31	10.37	447.11	
VNIR	701.10	10.51	447.21	
VNIR	707.95	11.11	465.61	
VNIR	714.87	10.60	447.29	
VNIR	721.86	9.60	405.14	
VNIR	728.92	8.29	373	
VNIR	736.03	9.84	404.36	
VNIR	743.21	10.47	426.81	
VNIR	750.45	10.38	414.75	
VNIR	757.74	10.30	410.56	

VNIR	765.09	5.67	286.84	
VNIR	772.49	9.85	390.78	
VNIR	779.94	9.80	374.06	485.48
VNIR	787.44	9.40	371.61	365.25
VNIR	794.99	9.05	350.73	365.99
VNIR	802.59	8.74	328.89	348.11
VNIR	810.23	8.48	321.57	337.57
VNIR	817.92	6.28	275.37	310.15
VNIR	825.65	7.56	292.83	310.9
VNIR	833.42	7.33	288.14	306.02
VNIR	841.23	8.15	294.19	311.5
VNIR	849.08	8.08	287.68	306.61
VNIR	856.96	8.16	284.01	307.3
VNIR	864.88	7.94	268.96	296.24
VNIR	872.82	7.89	265.36	296.22
VNIR	880.80	7.46	245.43	271.08
VNIR	888.79	7.53	246.1	265.19
VNIR	896.81	5.04	183.42	224.24
VNIR	904.85	6.14	197.32	243.07
VNIR	912.90	4.40	152.63	177.19
VNIR	920.96	5.47	171.71	223.18
VNIR	929.02	3.16	112.34	140.94
VNIR	937.10	0.82		62.17
VNIR	945.17	1.51		78.4
VNIR	953.25	1.79		85.55
VNIR	961.33	2.71	87.05	99.8
VNIR	969.41	4.78	122.04	147.61
VNIR	977.49	4.57	105.73	134.58
VNIR	985.58	5.30	115.16	137.17
SWIR	901.08	5.24	526.76	
SWIR	910.68	4.53	432.99	
SWIR	920.42	5.51	492.5	
SWIR	930.29	2.47	308.89	
SWIR	940.30	2.31	303.06	
SWIR	950.43	1.79	264.08	
SWIR	960.69	2.55	337.74	
SWIR	971.07	4.98	512.41	
SWIR	981.56	5.12	532	
SWIR	992.17	5.90	582.89	
SWIR	1002.90	5.81	590.18	
SWIR	1013.73	5.78	595.97	
SWIR	1024.66	5.64	594.82	
SWIR	1035.69	5.53	592.46	
SWIR	1046.82	5.35	589.19	
SWIR	1058.04	5.13	580.12	
SWIR	1069.34	4.80	564.46	
SWIR	1080.73	4.69	560.18	
SWIR	1092.19	4.35	538.34	
SWIR	1103.73	3.27	460.06	
SWIR	1115.34	1.17	241.93	
SWIR	1127.00	0.42	107.05	
SWIR	1138.73	1.32	270.52	
SWIR	1150.50	0.88	203.3	
SWIR	1162.31	2.47	404.84	
SWIR	1174.16	2.77	439.28	
SWIR	1186.04	3.31	491.72	
SWIR	1197.94	3.10	474.48	
SWIR	1209.87	3.25	490.04	
SWIR	1221.81	3.39	510.35	
SWIR	1233.76	3.60	528.99	
SWIR	1245.73	3.57	529.19	
SWIR	1257.70	3.25	508.55	
SWIR	1269.68	2.39	428.07	
SWIR	1281.67	3.00	491.31	
SWIR	1293.65	3.09	502.01	
SWIR	1305.62	2.58	456.42	
SWIR	1317.60	2.24	418.18	
SWIR	1329.56	1.10	273.92	
SWIR	1341.51	0.71	202.3	

SWIR	1353.44	0.01		
SWIR	1365.36	0.01		
SWIR	1377.25	0.01		
SWIR	1389.12	0.01		
SWIR	1400.97	0.01		
SWIR	1412.78	0.01		
SWIR	1424.56	0.04		
SWIR	1436.31	0.07		
SWIR	1448.02	0.30	101.88	
SWIR	1459.68	0.55	170.14	
SWIR	1471.31	0.11		
SWIR	1482.89	0.57	179.32	
SWIR	1494.43	1.13	294.74	
SWIR	1505.93	1.67	377.57	
SWIR	1517.39	1.84	404.09	
SWIR	1528.80	2.10	441.17	
SWIR	1540.17	2.15	449.31	
SWIR	1551.50	2.18	451.6	
SWIR	1562.78	2.15	446.35	
SWIR	1574.02	1.84	400.25	
SWIR	1585.21	2.02	431.82	
SWIR	1596.36	2.00	426.97	
SWIR	1607.46	1.81	407.28	
SWIR	1618.51	1.92	417.27	
SWIR	1629.52	1.94	428.04	
SWIR	1640.48	1.74	399.41	
SWIR	1651.39	1.75	401.5	
SWIR	1662.25	1.78	405.11	
SWIR	1673.07	1.73	400.66	
SWIR	1683.83	1.64	390.25	
SWIR	1694.55	1.65	392.68	
SWIR	1705.21	1.56	376.38	
SWIR	1715.83	1.49	369.69	
SWIR	1726.39	1.38	350.96	
SWIR	1736.91	1.21	329.98	
SWIR	1747.38	1.07	300.28	
SWIR	1757.80	1.05	298.65	
SWIR	1768.17	0.93	273.94	
SWIR	1778.49	0.59	199.14	
SWIR	1788.76	0.54	186.52	
SWIR	1798.98	0.19	76.4	
SWIR	1809.16	0.02		
SWIR	1819.29	0.00		
SWIR	1829.37	0.00		
SWIR	1839.41	0.00		
SWIR	1849.40	0.00		
SWIR	1859.34	0.00		
SWIR	1869.24	0.00		
SWIR	1879.09	0.00		
SWIR	1888.90	0.00		
SWIR	1898.66	0.00		
SWIR	1908.37	0.00		
SWIR	1918.05	0.00		
SWIR	1927.67	0.00		
SWIR	1937.26	0.00		
SWIR	1946.80	0.01		
SWIR	1956.29	0.02		12.1
SWIR	1965.74	0.16		91.07
SWIR	1975.15	0.33		159.68
SWIR	1984.52	0.61		234.68
SWIR	1993.85	0.57		228.72
SWIR	2003.13	0.06		41.28
SWIR	2012.37	0.12		68.66
SWIR	2021.57	0.27		140.18
SWIR	2030.73	0.60		236.96
SWIR	2039.84	0.66		250.64
SWIR	2048.92	0.50		212.51
SWIR	2057.96	0.39		176.83
SWIR	2066.95	0.39		176.46

SWIR	2075.91	0.58		230.54
SWIR	2084.83	0.65		249.89
SWIR	2093.70	0.71		260.88
SWIR	2102.54	0.72		264.83
SWIR	2111.34	0.72		260.64
SWIR	2120.11	0.71		260.12
SWIR	2128.83	0.73		265.94
SWIR	2137.52	0.73		266.51
SWIR	2146.17	0.73		265.04
SWIR	2154.78	0.66		251.7
SWIR	2163.36	0.62		243.27
SWIR	2171.90	0.65		250.83
SWIR	2180.41	0.63		243
SWIR	2188.88	0.60		237.72
SWIR	2197.32	0.56		224.48
SWIR	2205.72	0.57		226.06
SWIR	2214.08	0.61		234.64
SWIR	2222.42	0.62		238.55
SWIR	2230.72	0.60		235.02
SWIR	2238.98	0.59		229.79
SWIR	2247.22	0.56		223.61
SWIR	2255.42	0.54		219.27
SWIR	2263.58	0.52		213.68
SWIR	2271.72	0.52		212.82
SWIR	2279.82	0.51		208.05
SWIR	2287.90	0.51		208.99
SWIR	2295.94	0.47		198.68
SWIR	2303.95	0.46		195.86
SWIR	2311.92	0.51		209.11
SWIR	2319.87	0.37		168.28
SWIR	2327.79	0.44		189.5
SWIR	2335.67	0.41		182.68
SWIR	2343.52	0.34		160.93
SWIR	2351.35	0.29		140.3
SWIR	2359.14	0.35		162.81
SWIR	2366.90	0.31		145.59
SWIR	2374.64	0.26		132.36
SWIR	2382.34	0.23		118.95
SWIR	2390.02	0.24		122.49
SWIR	2397.66	0.27		129.98
SWIR	2405.28	0.22		113.34
SWIR	2412.86	0.17		94.82
SWIR	2420.42	0.17		87.89
SWIR	2427.95	0.23		115.94
SWIR	2435.45	0.13		66.25
SWIR	2442.92	0.20		101.93

Table 7-9 SNR values per wavelength for VNIR and SWIR low and high gains

Radiometric calibration updates

The following calibration products were generated and delivered:

Product	Type	Date of Generation	Date of Validity Start	Date of Validity End	Delivered to
ENMAP01-CTB_RAD-20250901T000000Z_V040100_20250829T131520Z	CTB_RAD	29.08.2025	01.09.2025	-	DIMS
ENMAP01-REF_SUN-20250901T000000Z_V040100_20250829T131520Z	REF_SUN	29.08.2025	01.09.2025	-	DIMS

Table 7-10 Generated radiometric calibration tables

7.5.4 Geometric Calibration

There have been no new geometric calibration tables generated in the reporting period.

Type of Calibration Table	ID of Calibration Table	Date of Generation	Date of Validity Start	Date of Validity End
None				

Table 7-11 Generated new geometric calibration tables

The performance of the geometric calibration table is assessed in chapter 7.6.3.

7.6 Internal Quality Control

7.6.1 Archive

Within the given time period (01.07.2025 to 30.09.2025), 2196 datatakes with a total of 20625 tiles were acquired and archived (remark: additional datatakes acquired during this period but for which the archiving is pending might be missing in the statistics).

The overall quality rating statistics are listed in Table 7-12, and in relation to the Solar Zenith Angle (SZA) in Table 7-13. Also these ratings are further detailed for the VNIR and SWIR detector in Table 7-14, showing a nominal performance rating for the given quality thresholds.

In addition, the rating for the atmospheric conditions for the scenes are depicted in Table 7-15. When setting the atmospheric quality rating in relation to the illumination conditions (i.e., large SZA) during data acquisition (Table 7-16), ~2% of the “reduced qualityAtmosphere” ratings and ~2.5% of the “low qualityAtmosphere” ratings can be related to low Sun angles / night time acquisitions. In addition, the “low qualityAtmosphere” rating can be further related to high cloud cover (53% of the low qualityAtmosphere tiles) and the unavailability of enough DDV pixels (64%) (see Table 7-17). Consequently, the rating is absolutely reasonable and can be explained.

Parameter	Value	Percentage	Number of tiles
overallQuality	Nominal	99,5%	20524
	Reduced	<0.1%	13
	Low	0.4%	88

Table 7-12 Overall quality rating statistics

Parameter	Number of tiles	Sub-Parameter	Number of tiles
overallQuality = Low	88		
		Thereof with SZA > 70°	81

Table 7-13 Overall quality rating in relation to Sun Zenith Angle (SZA)

Parameter	Number of tiles	Sub-Parameter	Number of tiles
overallQuality = Reduced	13		
		Thereof with qualityVNIR nominal	0
		Thereof with qualitySWIR nominal	13
overallQuality = Low	88		
		Thereof with qualityVNIR nominal or reduced	16
		Thereof with qualitySWIR nominal or reduced	71

Table 7-14 Reduced and low quality rating statistics

Parameter	Value	Percentage
QualityAtmosphere	Nominal	46%
	Reduced	11%
	Low	43%

Table 7-15 QualityAtmosphere rating statistics

Parameter	Number of tiles	Sub-Parameter	Number of tiles
overallAtmosphere = Reduced	2298		
		Thereof with SZA > 60°	44
		Thereof with SZA > 70°	20
		Thereof with SZA > 80°	4
overallAtmosphere = Low	8773		
		Thereof with SZA > 60°	223
		Thereof with SZA > 70°	136
		Thereof with SZA > 80°	85

Table 7-16 QualityAtmosphere rating in realtion to Sun Zenith Angle (SZA)

Parameter	Number of tiles	Sub-Parameter	Number of tiles
overallAtmosphere = Low	8773		
		Thereof with Cloud Cover > 66%	4716
		Thereof with DDV warnings	5643

Table 7-17 QualityAtmosphere rating in relation to Cloud Cover and DDV availability

Remark about definition of EnMAP low quality collection

The quality rating of EnMAP products is based on image parameters, such as illumination conditions (i.e., sun elevation angle) and image defects, and on possible anomalies in the image data or instrument telemetry. These parameters are retrieved during the pre-processing and are added to the metadata and quality layers for every archived L0 product. In EOWEB GeoPortal two collections of EnMAP L0 products are available: “EnMAP-HSI (L0)” and “EnMAP-HSI (L0), Low Quality”. An L0 product is assigned to the low-quality collection if the corresponding metadata item qualityFlags.overallQuality is equal to 2 (low quality). This happens for products with a significant number of striping, saturation, artefact or dead pixels, when the screening of data and instrument indicates non-nominal behavior or, in the majority of cases, when the sun elevation angle is less than or equal to 0 (e.g., night scenes). A detailed definition of qualityFlags. overallQuality is given in Sec. 4.4.9 in the L1B ATBD (EN-PCV-TN-4006).

7.6.2 Level 1B

7.6.2.1 Radiometric Performance

Defective / de-calibrated detector elements

Using the Detector Map components, an offline check of possibly defective or de-calibrated detector elements is conducted. In particular, a detector element is identified as “possibly defective” if it is suspicious in at least 75% of the useful tiles. Note that this analysis is based on L1B_RAD data, so no dead / defective pixel interpolation was carried out. Within the given reporting period, the following indications for defective pixels are found for the VNIR and the SWIR camera:

VNIR (total of 16021 tiles, with 15891 suitable for analysis):

Newly found suspicious pixels in green, previously detected in **black**, no longer present ones in ~~red~~.

Band	Cross-track element
~~19~~	~~187~~
77	600
85	14
89	395

Note that the band index starts at 1.

SWIR (total of 16021 tiles, with 15782 suitable for analysis):

Newly found suspicious pixels in green, previously detected in **black**, no longer present ones in ~~red~~.

NOTE: due to the change in SWIR band configuration within the period Q3 2023, the band index from band 45 till 75 did change by +1 (with bands 45, 74 & 75 newly added) w.r.t. the reports before Q3 2023.

Band	Cross-track element
1	817
2	235, 286, 593, 673
3	381
4	362, 363, 418
5	687
7	472, 910
8	801
9	124
11	715
14	29, 684
16	535
~~20~~	~~84~~
~~28~~	~~104~~
29	928
30	360, 855
31	360

Band	Cross-track element
33	560
38	241, 919
48	511
50	311, 344, 395
53	97, 98
54	941
56	221, 965
58	632, 667, 922
59	89, 90
61	312
63	123
66	93
69	864
72	801, 845
75	737

Band	Cross-track element
85	525
89	285
91	973
92	677, 973
96	341, 819
~~100~~	~~513~~
101	318
~~102~~	~~925~~
106	107
107	265, 764
108	886
111	315
118	837

Dead detector elements

Within the given reporting period, the statistics for dead pixels are provided in Table 7-18 and Table 7-19. When comparing these numbers to the estimates in Ch. 7.5.1, one must bear in mind that the latter is based on the full detector readout configuration, while the numbers provided in the following are related to the standard readout configuration as provided in the user product. Because of the smaller readout area, these following dead pixel numbers are lower in comparison.

Parameter	Number of dead pixels	Percentage of tiles in reporting period
DeadPixelsVNIR	137	100%

Table 7-18 Dead pixel statistics, VNIR

Parameter	Number of dead pixels	Percentage of tiles in reporting period
DeadPixelsSWIR	1509	100%

Table 7-19 Dead pixel statistics, SWIR

Saturation and radiance levels

Within the given reporting period, no indications for increased saturation defects are found for the VNIR and the SWIR camera (see Table 7-20 and Table 7-21).

Parameter	Value (per mille of scene)	Percentage of tiles
SaturationCrosstalkVNIR	0	91%

	> 0 per mille	9.1%
	> 10 per mille	1.7%

Table 7-20 Saturation statistics, VNIR

Parameter	Value (per mille of scene)	Percentage of tiles
SaturationCrosstalkSWIR	0	92%
	> 0 per mille	7.8%
	> 10 per mille	0.4%

Table 7-21 Saturation statistics, SWIR

Other radiometric artifacts

Within the given reporting period, the striping performance is similar to the one encountered during the Commissioning Phase. Within PCV, different de-striping approaches were tested, and the selected one by M. Brell (GFZ) is implemented in processor version V01.02.00 (07.03.2023).

Apart from this, no indications for an increase in general radiometric artifacts are found for the VNIR and the SWIR camera (see following tables).

Parameter	Value (number of pix)	Percentage of tiles
generalArtifactsVNIR	0	0%
	> 0	100%
	> 10	4.9%
	> 100	0.6%
	> 1000	0%

Table 7-22 Artifacts statistics (without striping), VNIR

Parameter	Value (number of pix)	Percentage of tiles
generalArtifactsSWIR	0	0%
	> 0	100%
	> 10	100%
	> 25	2.6%
	> 100	0.5%
	> 1000	0%

Table 7-23 Artifact statistics (without striping), SWIR

7.6.2.2 Spectral Performance

For the analysis of the spectral stability, the Detector Maps of all Earth datatakes acquired in the reporting period were used. Note that no smile correction was applied, so the analysis shows only on the instrument characteristics. At the wavelengths of stable atmospheric features (760 nm Oxygen absorption and CO2 absorption at ~2050 nm), simulations of spectral shifts were carried out by resampling the absorption in the interval of +/- 3.0 nm with steps of 0.05 nm. Then the signal of the Detector Maps and the simulated shifted absorptions were normalized, and a least-square fit was used where the sensed absorption matches the simulations. Also an additional polynomial fitting was applied, as especially the CO2 absorption band region has low signal an is thus significantly influenced by noise.

For the VNIR, when aggregating the shifts (Figure 7-18) the mean derivation is almost constant in across-track direction and -as before- around 0.5 nm towards shorter wavelengths, underpinning the consistency with the in-orbit spectral calibration and especially regarding the shape of the spectral smile. Note that of course these results are consistent within the limitations of this vicarious approach. Additionally, the variability of the vicariously estimated spectral calibration can be expressed as the standard deviation at 1 sigma is below 0.3 nm, which includes the spectral stability of EnMAP and as well the variations of the used Earth datatakes and the limitations of the method.

In summary, for the VNIR the estimated differences to the CTB_SPC consistent with the results of previous reporting periods, confirming the validity of the spectral calibration and the spectral stability of the instrument taking into accounts the limitations of the vicarious approach.

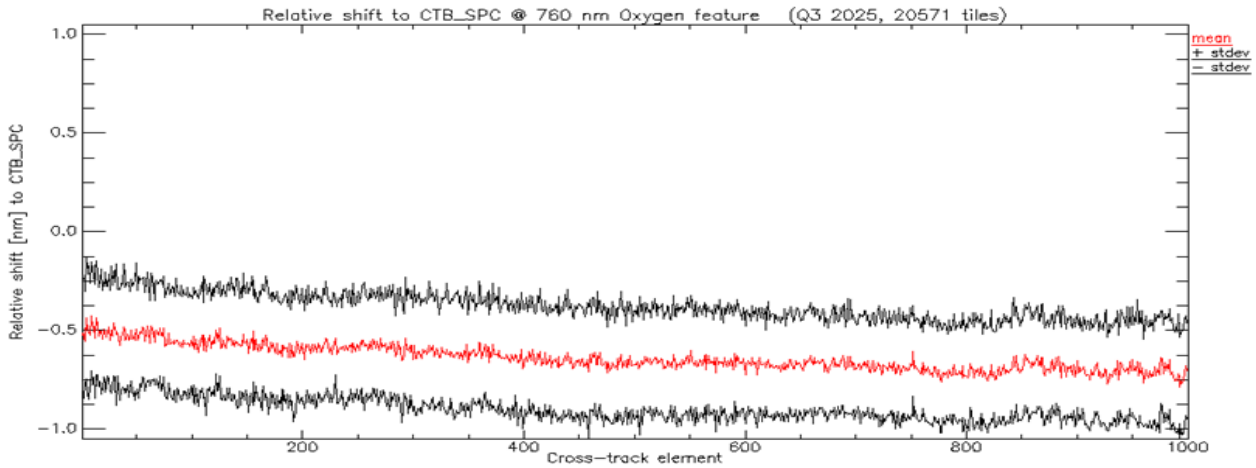

Figure 7-18 VNIR estimated spectral shift at 760 nm w.r.t the valid spectral calibration table (CTB_SPC), and relative spectral stability expressed at 1 sigma (Q3 2025, 15920 tiles)

For this analysis, the reference is thus not the nominal center wavelengths (i.e., a single number per band), but the CW per cross-track pixel, thus explicitly including the spectral smile (see Figure 7-19).

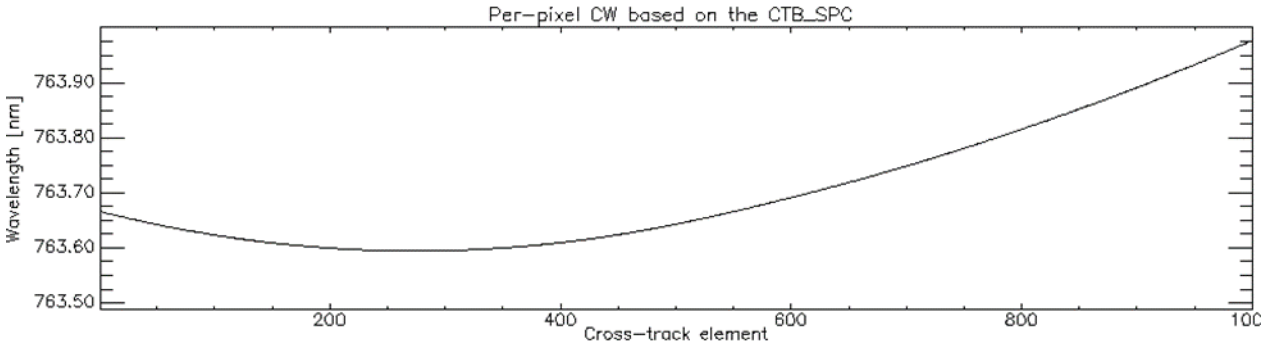

Figure 7-19 Center wavelengths per cross-track pixel based on the spectral calibration table (VNIR band 62) in the calibration table (CTB_SPC).

For the SWIR having less pronounced atmospheric absorption features, more influence of the background and a much lower signal level, the fitting also results in more clutter, as shown in Figure 7-20.

In order to demonstrate that the mean derivation to the CTB_SPC is within the spread of the data, the mean and standard deviation are calculated using the relative values, as shown in Figure 7-20. For Q3 2025, a small shift of ~0.4 nm towards longer wavelengths is visible when comparing to CTB_SPC (Figure 7-21). This shift is equal for all cross-track elements, so the shape of the spectral smile did not change and is well represented in the CTB_SPC. When comparing this small spectral shift to the results in the past quarter, the tendency towards longer wavelengths by ~0.4 nm was also present, but then with a larger magnitude and within a larger clutter in the fitted data. In addition, the spread around the estimated mean with a

standard deviation of ~0.5 nm (1 sigma) indicates no significant change of the good overall stability of the instrument.

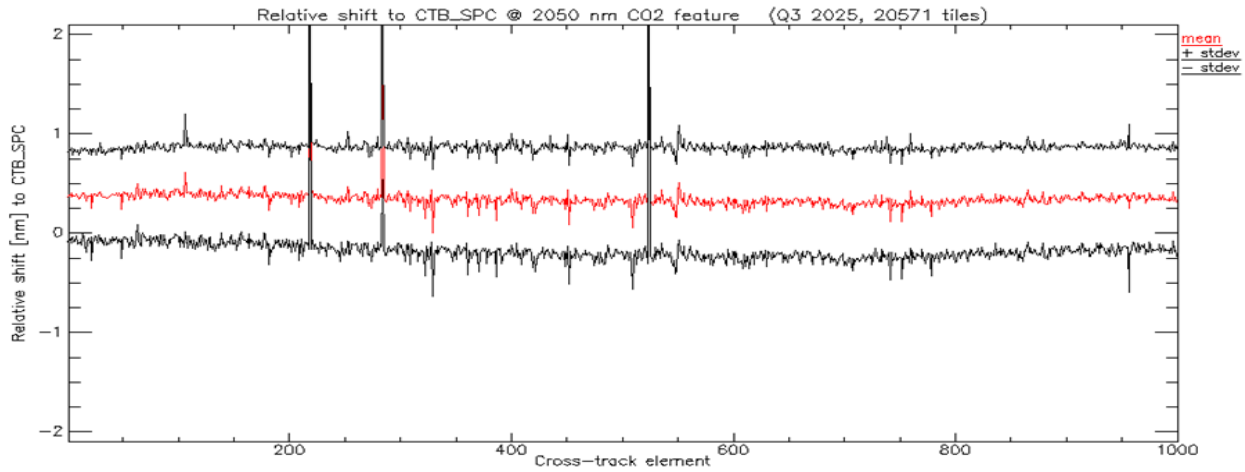

Figure 7-20 SWIR estimated spectral shift at 2050 nm w.r.t the valid spectral calibration table (CTB_SPC, shown below), and relative spectral stability expressed at 1 sigma (Q3 2025, 17894 tiles)

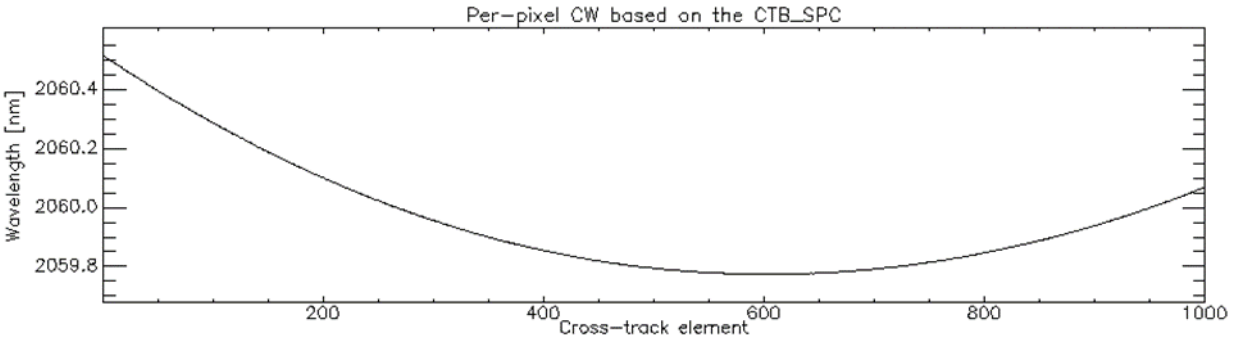

Figure 7-21 Center wavelengths per cross-track pixel based on the spectral calibration table (SWIR band 86).

7.6.3 Level 1C

This report covers the timeframe from 01.07.2025 to 30.09.2025. No geometric calibration was performed during this period.

In the timeframe of this report, 2176 datatakes have been acquired. In 1586 of those datatakes (~73 %), enough ground control points (GCP) and independent check points (ICP) were found to perform a geometric accuracy assessment. The datatakes without enough GCPs were not assessed quantitatively, but a random subset of them was inspected visually. The vast majority of those datatakes was either almost fully covered with clouds or showing only water, desert or rain forest. The behavior is thus as expected.

The assessment of the RMSE values in the metadata is shown below in Figure 7-22.

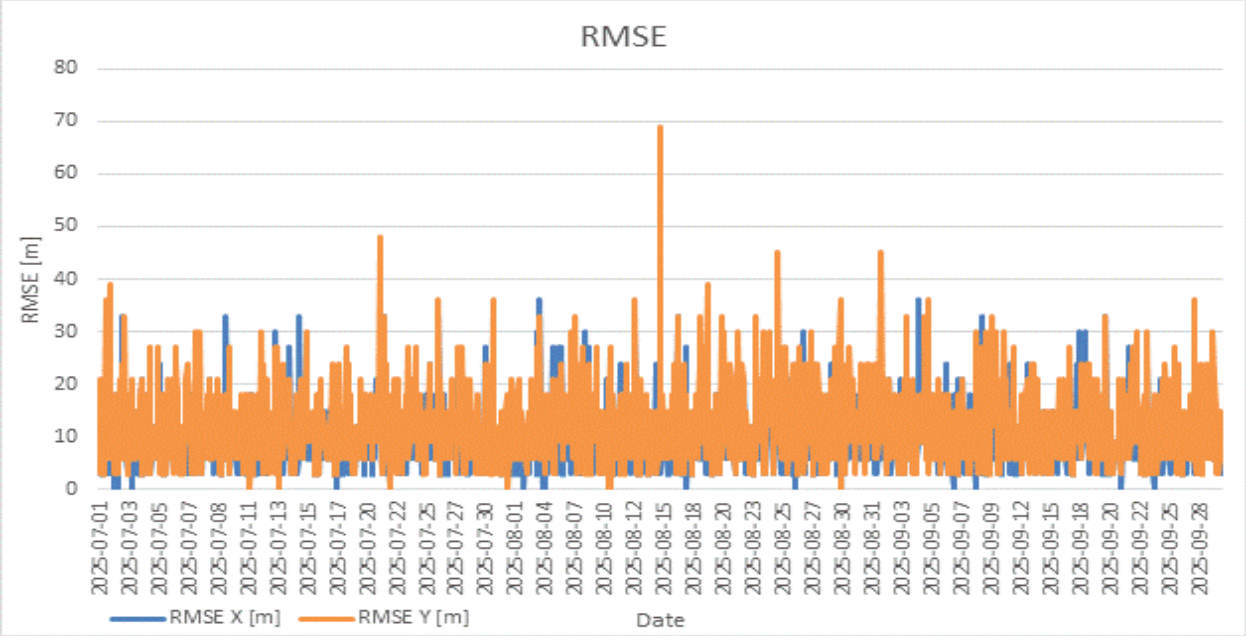

Figure 7-22 Assessment of RMSE values, calculated based on found ICPs, for all datatakes where ICP could be found

In x-direction, 11 datatakes (~0.7%) had an RMSE value above 30 m (1 GSD), whereas in y-direction, 26 datatakes (~1.6%) are above this threshold. For most of those datatakes, only very few GCP and ICP could be found during processing, making the results less reliable. The mean values are 9.43 m in x-direction and 12.01 m in y direction. This shows a very high geolocation accuracy for the datatakes where matching was possible. The requirement GRD-PCV-0155 (1 GSD) is thus fulfilled.

The average boresight angles, which can be interpreted as the correction and thus the error of the scene if no GCPs could have been found, correspond to approximately -15 m in x direction with a standard deviation of approximately 22 m and -31 m in y direction with a standard deviation of approximately 23 m on ground. It is reasonable to assume that the scenes where no GCPs could be found are in the same accuracy range and thus well within the requirement of 100 m (GRD-PCV-0150). Note that the x and y direction mentioned in this report are not in the image coordinate system but in UTM, as the evaluation is done on L1C products..

7.6.3.1 **Geometric accuracy**

EnMAP L1C products are matched against a reference image (Sentinel-2 data, if not stated otherwise) by using image matching techniques to assess the geometric accuracy. At the obtained checkpoints (CP), statistics are calculated to provide mean and RMSE values (Figure 7-23) for each scene. Note that the obtained accuracy in the analysis is always w.r.t. the reference image. This report covers EnMAP data from 01.07.2025 to 30.09.2025. A random sample of 562 L1C tiles was selected based on visual inspection of the catalogue quicklooks (e.g. to avoid cloudy images).

The requirement GRD-PCV-0155 shall be fulfilled:

The geolocation accuracy at nadir look direction of level 1C and 2A products shall be better than 1 GSD (1 sigma) in each direction with respect to reference images provided that reference images are available and sufficient similarity.

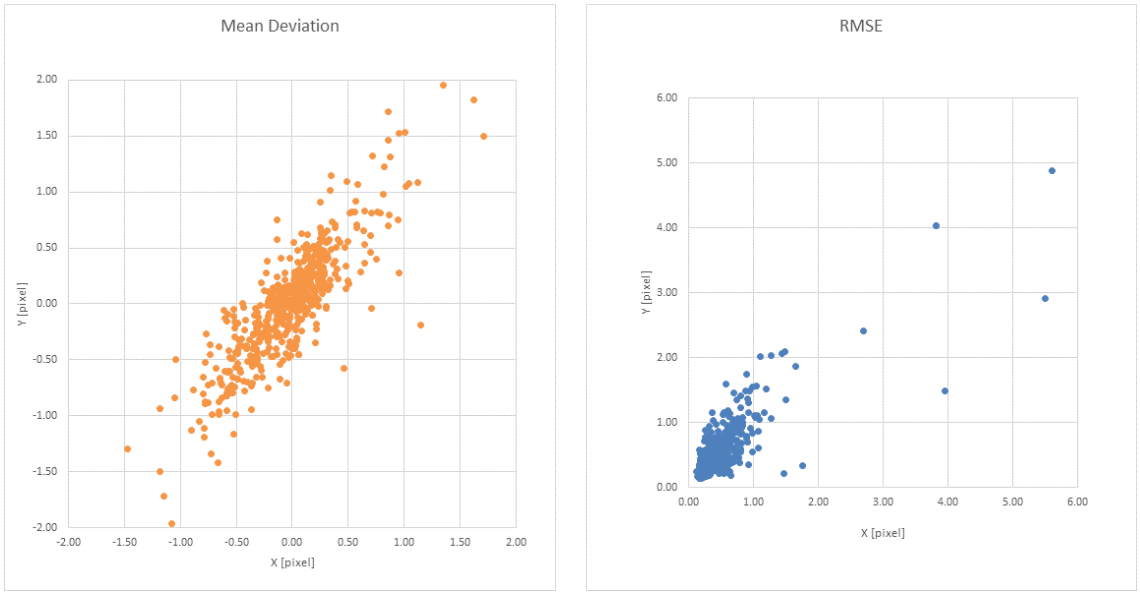

Figure 7-23 Mean deviation of EnMAP L1C products in pixel (left). RMSE value for EnMAP L1C products in pixel (right)

Note, that during processing the boresight angles and the geometric accuracy related quality flags are calculated on datatake level while in the figures and tables above, the accuracy is assessed per tile. The mean values over all 562 L1C tiles are -0.03 and 0.00 pixel in mean deviation with a standard deviation of 0.46 and 0.60 pixel while the mean RMSE values are 0.49 and 0.55 pixel, all in x and y direction respectively. The data show that for the vast majority of scenes the accuracy wrt. reference image is better than one pixel and thus the requirements are fulfilled. Compared to the last geometric QC report, the values are very stable (see Figure 7-25).

7.6.3.2 **Co-registration accuracy**

In this section, the co-registration accuracy is checked against the Space Segment requirement SRDS-PIM-0050 (EN-KT-RFW-003 is also to be considered here):

*The HS-Imager shall be designed such, that the geometric co-registration is ≤ 20 % of the nominal Ground Sampling Distance (0.2 * GSD linear displacement in both directions).*

For the assessment of co-registration accuracy, the SWIR data of EnMAP L1C products are matched against the corresponding VNIR data and the mean deviation values shown in this section (Figure 7-24).

This report covers EnMAP data from 01.07.2025 to 30.09.2025. A random sample of 565 L1C tiles was selected based on visual inspection of the catalogue quicklooks (e.g. to avoid cloudy images).

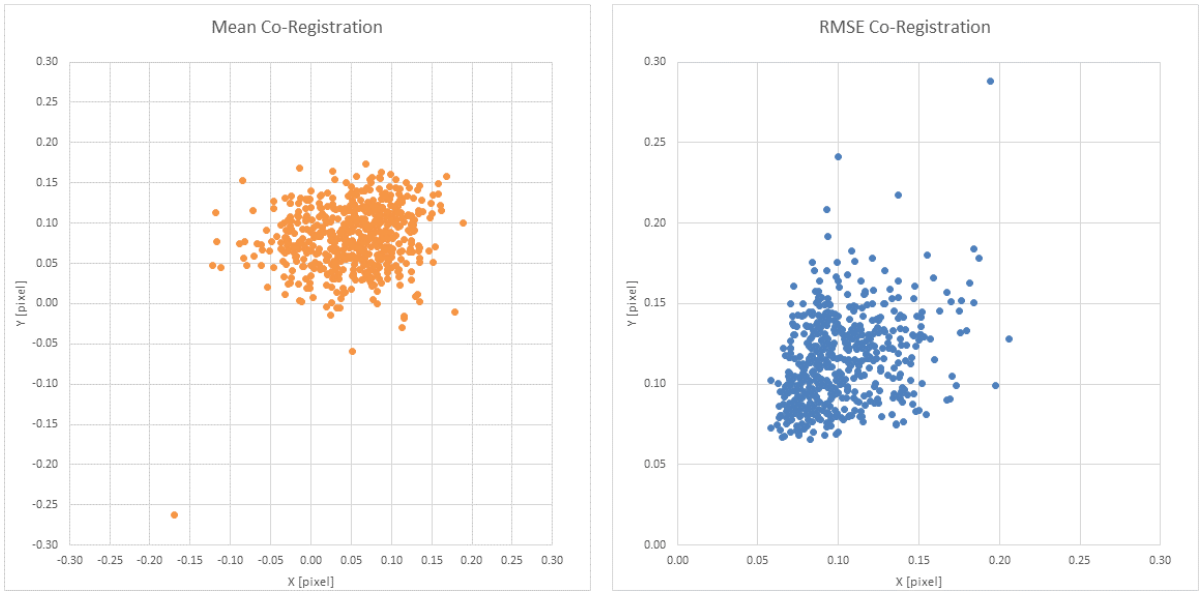

Figure 7-24 Mean deviation in pixel between VNIR and SWIR data of EnMAP L1C products (left). RMSE in pixel between VNIR and SWIR data of EnMAP L1C Products (right)

The data show, that the mean co-registration is well within the requirement. Note that the theoretical accuracy of the used matching algorithm is 0.1 pixel, and as can be seen in the RMSE values, still some mismatches were not removed by the blunder detection techniques that were applied. The mean deviation over all analyzed tiles are 0.05 pixel in x-direction with a standard deviation of 0.05 pixel and 0.08 pixel in y direction with a standard deviation of 0.04 pixel. Compared to the results in the previous geometric QC report, the values are very stable as can be seen in Figure 7-25.

7.6.3.3 **Development of geometric performance**

Since the launch of EnMAP on April 1st 2022, the geometric performance has been improved significantly. This was achieved by different geometric calibrations and processor updates. Table 7-24 shows the measures performed, their date and their effect.

Date	Measure	Effect
01.08.2022	Fix of attitude processing	Improvement of absolute geolocation (w/o matching)
20.09.2022	Boresight Calibration	Improvement of absolute geolocation (w/o matching)
03.11.2022	1st Geometric Calibration	Improvement of absolute geolocation (w/o matching) Improvement of VNIR/SWIR co-registration (~0.8 pix -> ~0.4 pix)
11.02.2023	2nd Geometric Calibration	Improvement of VNIR/SWIR co-registration (~0.4 pix -> ~0.15 pix)
29.03.2023	Processor update (v01.02.00)	Improvement of VNIR/SWIR co-registration (~0.15 pix -> ~0.06 pix)

Table 7-24 Improvement of geometric performance

Figure 7-25 shows the development of the co-registration accuracy, measured as described in previous section. Again, after a significant improvement since commissioning phase, over the last report periods the accuracy has been very stable.

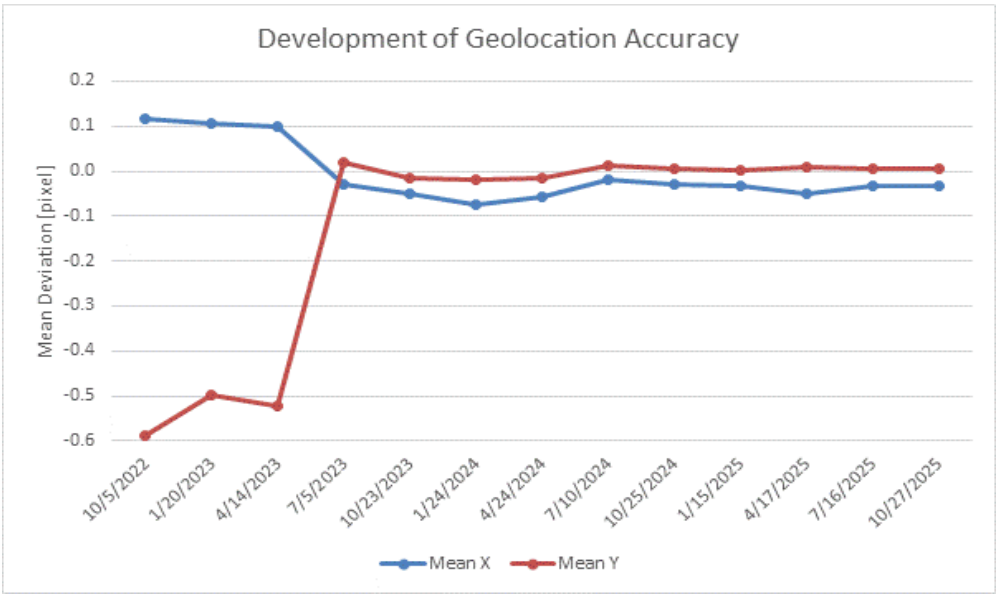

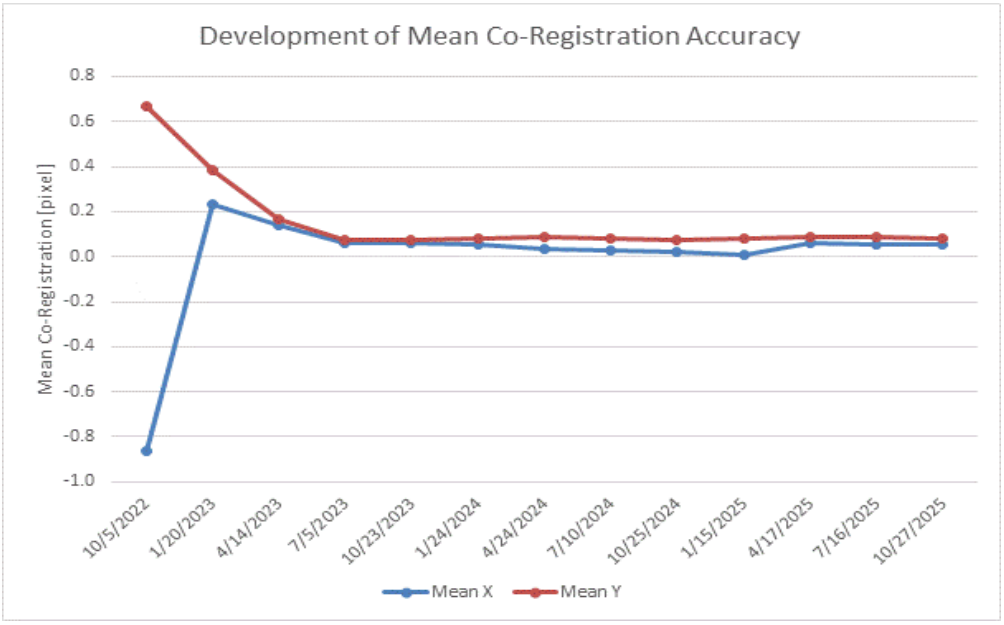

Figure 7-25 Development of co-registration accuracy based on the previous geometric QC reports

As most of the geometric processing – especially the matching against a reference image – is done on datatake level during L0 processing, the geometric accuracy and co-registration of data acquired earlier during the mission is not automatically improved when higher level products (L1B, L1C, L2A) are processed with the current processor version. However, after completing the L0 reprocessing of the whole archive, the geometric processing is executed with the latest processor version and geometric calibration table to make sure that the best geometric quality and co-registration is reached also for the reprocessed data. Today, the geometric performance of the products available in the Mission Archive with date earlier than 29.03.2023 is the same as for the products acquired after that date. Users can recognize reprocessed data by checking the metadata tag **archivedVersion**: if the version is 01.03.00 or higher, then the geometric performance should be as analyzed in this report, regardless of the acquisition date of the product.

7.6.4 Level 2A

7.6.4.1 **Validity of generated L2A "water" data**

7.6.4.1.1 Analyzed scenes

The following scenes were taken into consideration:

DataTake - ID	Tile - ID	Location	L2A Option	Cirrus / Haze Removal	Overall Quality
150867	04	AUS, Dunwich	Water mode, water type "clear"	Cirrus	Nominal
147903	02	ITA, Venice	Water mode, water type "clear"	Cirrus	Nominal
149727	21	DE, Fehmarn	Water mode, water type "clear"	Cirrus	Nominal
146798	02	ITA, Lake Trasimeno	Water mode, water type "clear"	Cirrus	Nominal
148819	07	AT, Plansee	Water mode, water type "clear"	Cirrus	Nominal

Table 7-25 Datatake IDs of analyzed water products

The below listed parameters were checked for above mentioned scenes by EOMAP:

Parameter	Check
Masking (Land, Water, Clouds, etc.)	No issues found.
Adjacency correction	No issues found.
Retrieval of atmospheric properties	No issues found.
Cirrus – correction	No issues found.
Retrieval of water leaving reflectance	No issues found.
Quality Mask	No issues found.

7.6.4.1.2 Data Checks

For the checks described in the following, multiple scenes were used. The corresponding scene - IDs and locations can be found in Table 7-25.

- Masking

First, the geo mask is checked. The different parts of the scene shown masked (see Figure 7-26 and Figure 7-27) are classified as expected.) are classified as expected.

Figure 7-26 Scene-ID 147903; RGB-Quicklook with Bands 611.02nm – 550.69nm – 463.73nm

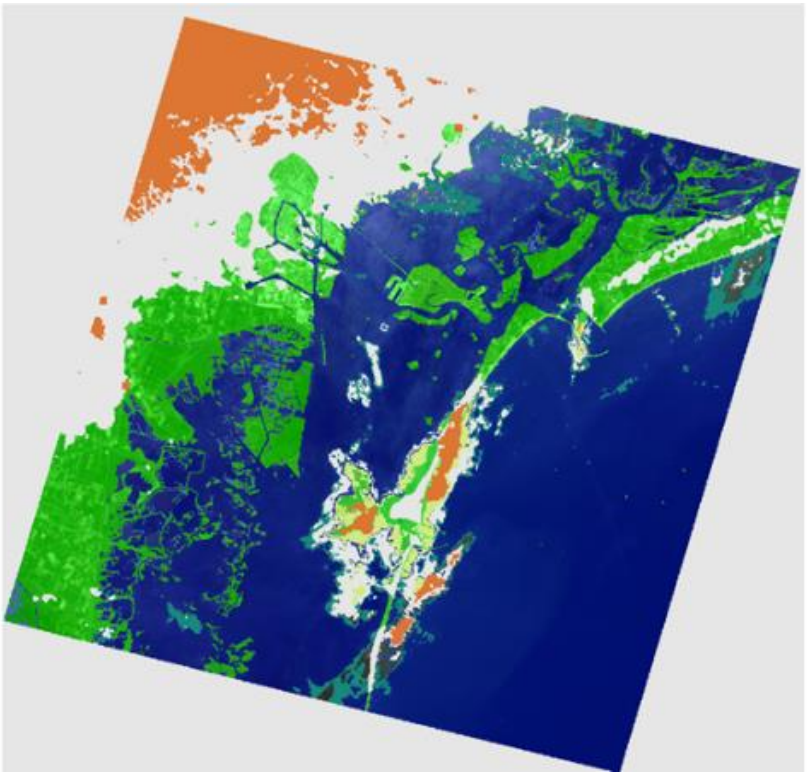

Figure 7-27 Scene-ID 147903; Geo Mask with Blue – Water, Green – Land, Orange – Clouds, Red – Cloud Shadow, Dark Green – Cirrus, White – NA

- Cirrus and Adjacency Correction

Next, we check for the cirrus and adjacency correction using the two sites ‘AC1’ and ‘AC2’ shown in Figure 7-26.

The coordinates of the sample locations are as follows:

AC 1: LAT 45.41504061 | LON 12.38306748

AC 2: LAT 45.35260096 | LON 12.42380281

For sampling, we choose two locations, one located over shallow water, the other over deep water (see Figure 7-26 for the sample locations).

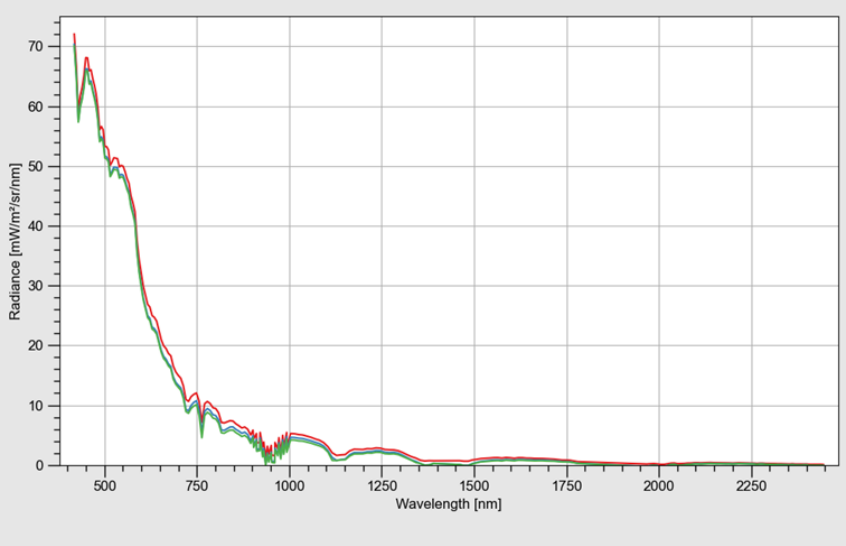

Figure 7-28 Scene-ID 147903; At-sensor-radiance sampled at location AC 1; red: measured, blue: cirrus corrected, green: adjacency corrected. Note that the blue line is close to the green one.

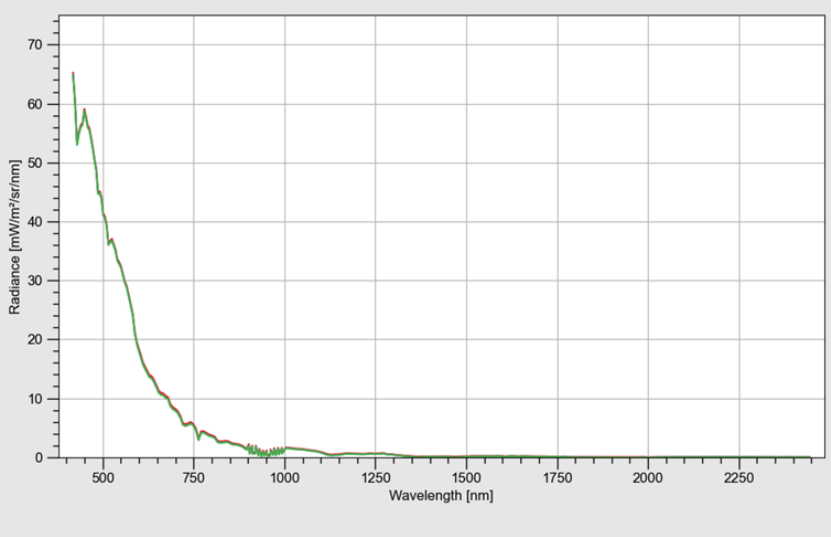

Figure 7-29 Scene-ID 147903; At-sensor-radiance sampled at location AC 2; red: measured, blue: cirrus corrected, green: adjacency corrected. Note that the blue and green lines are almost identical.

Figure 7-28 and Figure 7-29 depict the sampled at-sensor-radiance - signal for location AC 1 and AC 2, respectively. As it can be seen, the adjacency correction sampled at AC 1 has a slightly stronger influence compared to the one sampled at AC 2. This is what we would expect, since AC 1 is located directly next to some very bright land part, thus the signal sampled over water is supposed to be much more affected. Before the adjacency correction takes place, in this case the at-sensor-signal is corrected for the effect of cirrus clouds present in the scene (see Figure 7-27).).

- Reflectance Product

To get a better impression of the product normalized water leaving reflectance as the final one, Figure 7-30 shows the reflectance using the RGB channels 611.02nm, 550.69nm and 463.73nm. shows the reflectance using the RGB channels 611.02nm, 550.69nm and 463.73nm.

Figure 7-30 RGB-Quicklook (Radiance) of scene-ID 146798; Wavelengths for RGB: 611.02nm – 550.69nm – 463.73nm

Figure 7-31 Normalized Water Leaving Reflectance of scene-ID 146798; Wavelengths for RGB: 611.02nm – 550.69nm – 463.73nm

For the labeled location in Figure 7-30, the sampling coordinates is as follows:, the sampling coordinates is as follows:

nWLR: LAT 43.16028692 | LON 12.04699461

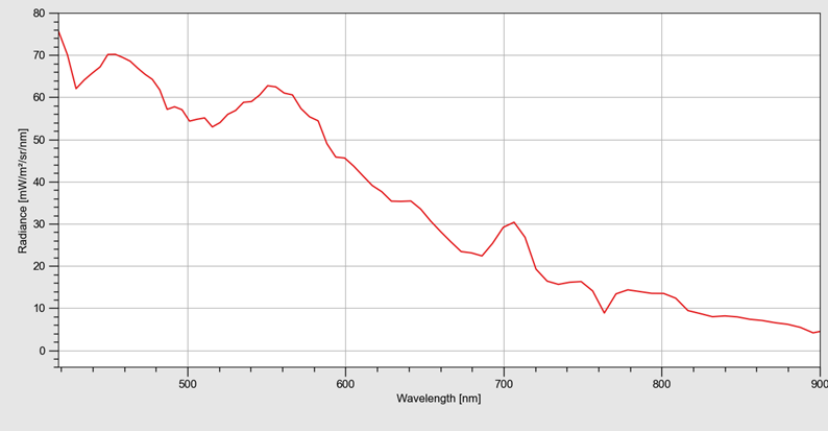

Figure 7-32 Scene-ID 146798; At-sensor-radiance sampled at location nWLR

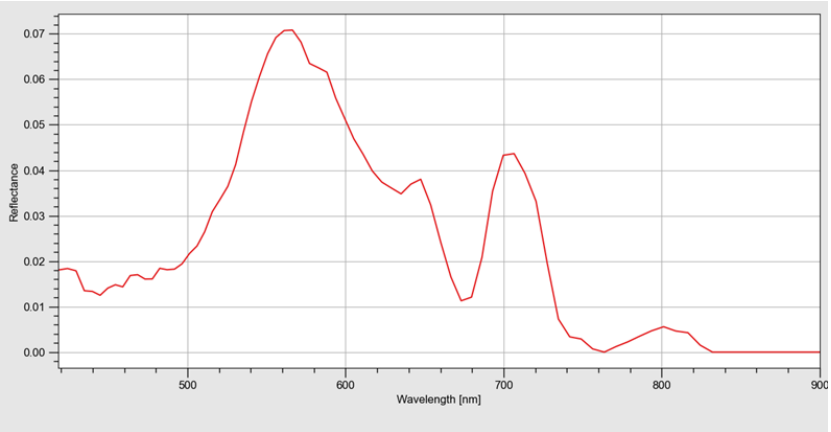

Figure 7-33 Scene-ID 146798; nWLR sampled at location nWLR

Figure 7-32 depict the at-sensor-radiance sampled at location nWLR1. Figure 7-33 shows the corresponding normalized water leaving reflectance (nWLR). As can be seen in Figure 7-30, the lake under investigation holds a highly concentrated load of probably organic substances. This assumption is confirmed by studying the signal plotted in Figure 7-33, especially by the (rough) spectral ranges between 400nm and 500nm, 640nm and 700nm, respectively. Furthermore, the value-add of nWLR as the final product of the atmospheric correction over water is visualized by comparing Figure 7-32 and Figure 7-33. While the at-sensor-radiance suffers still from the atmospheric influence, the nWLR is corrected for those parts of the signal and is thus dominated by the actual water constituents.

Summing up, the atmospheric correction workflow works as intended.

7.6.4.2 **Validity of generated L2A “land” data**

7.6.4.2.1 Analyzed scenes

Within the time interval between 01.07.2025 to 30.09.2025, an interactive in-depth analysis has been conducted for the following scenes:

Datatake-ID	Tile-ID	date	location	L2A option	cirrus and haze removal	Archived Version	processor version	Overall Quality	Quality Atm
141177	001	2025-07-07	Nevado Auzangate region, southeast Peru	land	no	01.05.02	V010502	Reduced	Reduced
148217	011	2025-08-20	Cape Range, western Australia	land	no	01.05.02	V010502	Nominal	Nominal
151218	004	2025-09-01	Bogs & forests in western Siberia north of Tomsk, Russia	land	no	01.05.02	V010502	Nominal	Nominal
145125	012	2025-08-01	Rio Grande dam, US-Mexican border	land	no	01.05.02	V010502	Nominal	Reduced

Table 7-26 Datatake IDs of analyzed land products

For the selection of L2A data, several data takes acquired within the reporting period and covering different landscapes at different conditions were analyzed.

7.6.4.2.2 Data Checks

In the following, the different tiles were checked for the shape and magnitude of the BOA_ref spectra, and also the quality of the generated masks is evaluated when meaningful.

For all tiles the visual image impression is fine. For the masking, there are known issues of mis-classifications which are currently being investigated. The BOA_ref spectra all show the typical shape and magnitude, indicating the correct L2A correction.

- **High alpine scene, Nevado Auzangate region, southeast Peru (DT141177, 2025-07-07)**

This investigated scene can be considered as atypical and “extreme”, as it has an average scene altitude of 4700 m a.s.l. (peaks even above 6300 m a.s,l) and very rough terrain. Also, multiple surface types like vegetation, rocks, glaciers as well as different water bodies are included. Due to the scene conditions, both the overall and the atmospheric quality rating are “reduced”.

When checking the shape of the spectra (Figure 7-34), the overall smooth shape and magnitude for all surfaces is as expected, but the snow/ice spectra show atypical spikes which are related to a known L2A issue which shall be fixed within the new processor version 01.05.05.

Considering the topographic correction (Figure 7-35), the effects are well corrected giving a “flattened” image impression without artefacts. The effects are well corrected giving a “flattened” image impression without artefacts.

For the masking (Figure 7-36), the snow mask is correct, but the clouds and cirrus are overestimated. Considering the mean scene elevation of 4700 m a.s.l., the general issue of masking of too many cirrus and clouds is known. But for this scene, the vast number of masked clouds will be further investigated.

Overall, the L2A results are as expected, with good surface reflection retrieval for all land and lake surfaces except snow/ice (fixed in upcoming processor version), a well-performing terrain correction, and the mentioned limitations of the physically-based cloud masking at very high terrain altitudes.

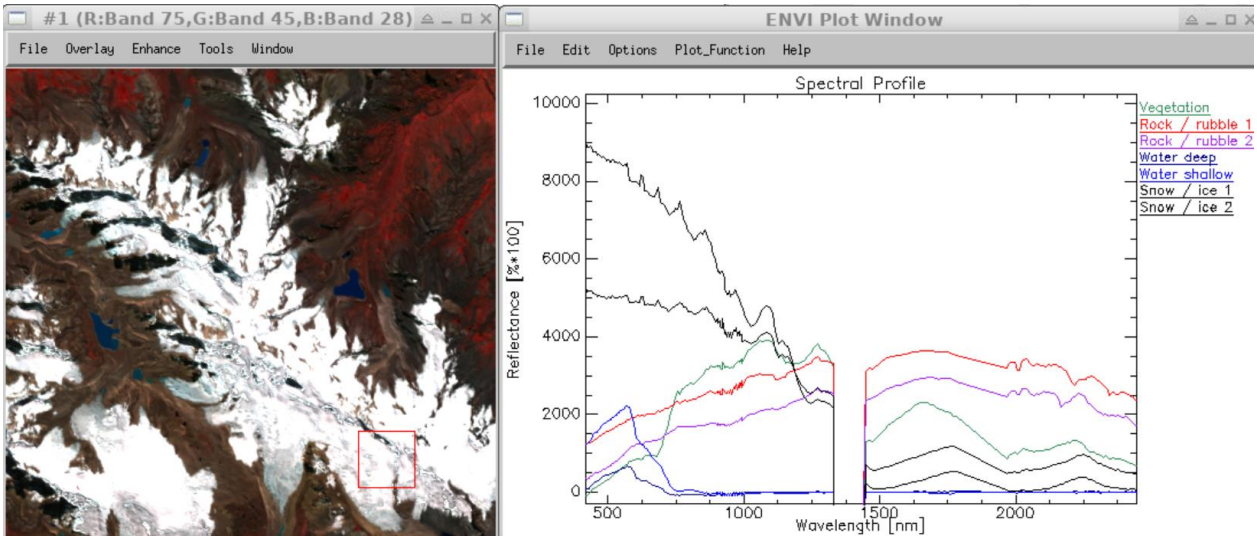

Figure 7-34 DT1411777_001, CIR image (subset), and single pixel spectra of various surfaces (L2A land processor).

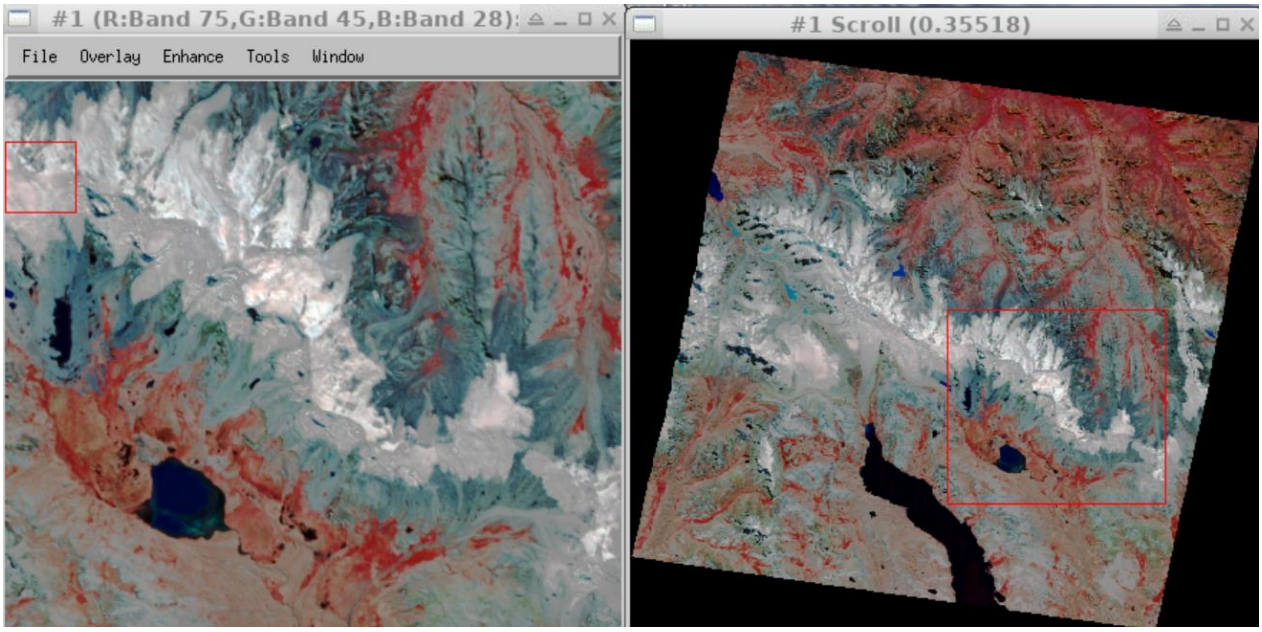

Figure 7-35 DT1411777_001, CIR image, gaussian stretch to highlight the accurate terrain correction

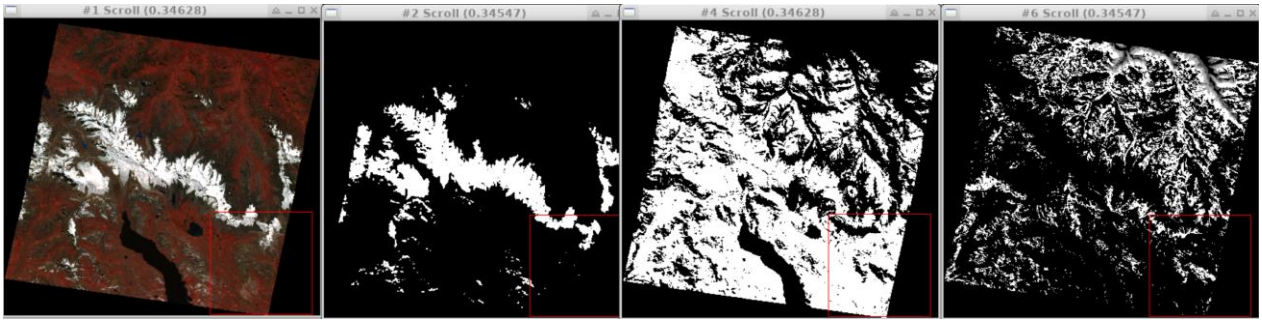

Figure 7-36 DT1411777_001, from left to right: CIR image, snow mask, cloud mask, cirrus mask (grey hues indicate thick - medium - thin cirrus). Note that haze and cloud shadow masks are correctly empty and thus not depicted.

- **Cape Range, western Australia (DT148217, 2025-08-20)**

The scene of the Cape Range peninsula includes land, coastal and deep water, and also many small clouds. As can be seen in Figure 7-37, the masking for this scene is generally challenging. Close to the coast, haze over land and water is detected; within some of these haze-affected areas, the bright sands are masked as “snow”, while all other bright sands are correctly excluded. Thus, this incorrect “snow” flag for some areas can be related to the uncorrected influence of the haze (processing option was following the GEOSERVICE standard, thus having no haze correction).

Clouds are generally well detected with some thin clouds and also thinner cloud edges missing, as shown in (Figure 7-38). Additionally, the cloud shadow mask is missing out many shadow areas for this scene. This shortcoming of the current masking approach is well known, and thus the performance is as expected.

The related ground reflectance spectra (Figure 7-39) over land and water are all as expected in shape and magnitude, and include the well-known “zig-zag” in the VNIR-SWIR overlapping region originating in the radiometric calibration.

To summarize, the performance of the L2A processing for this scene is as expected.

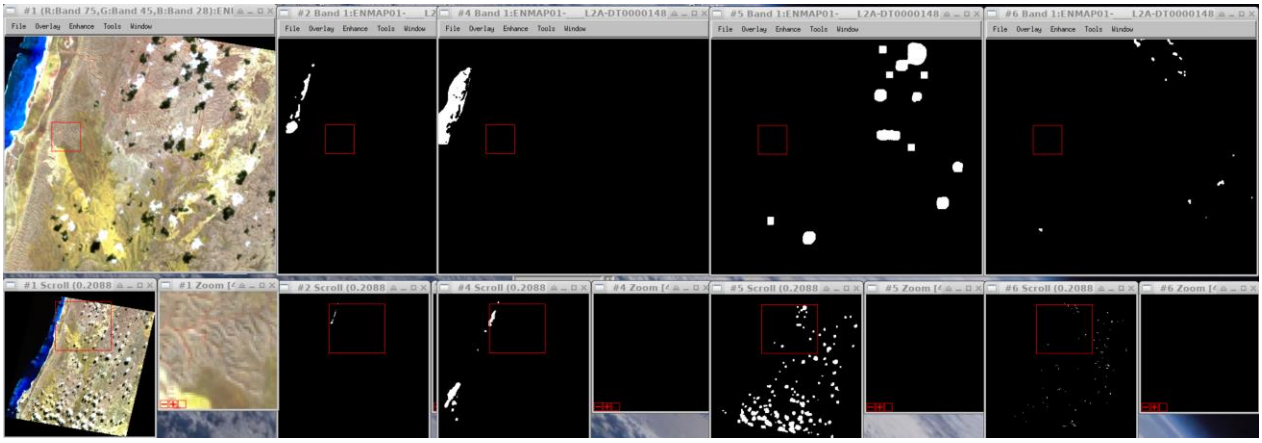

Figure 7-37 DT148217_011, left to right: CIR image, snow mask, haze mask, cloud mask, cloud shadow mask (sidenote: cirrus mask not provided as no cirrus were flagged).

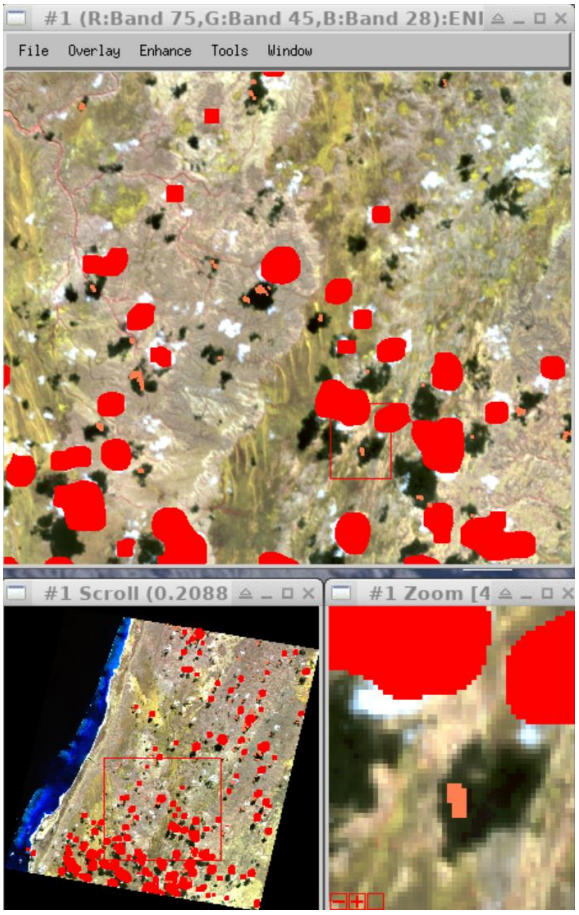

Figure 7-38 DT148217_011, CIR image overlayed with cloud mask (red) and cloud shadow mask (orange)

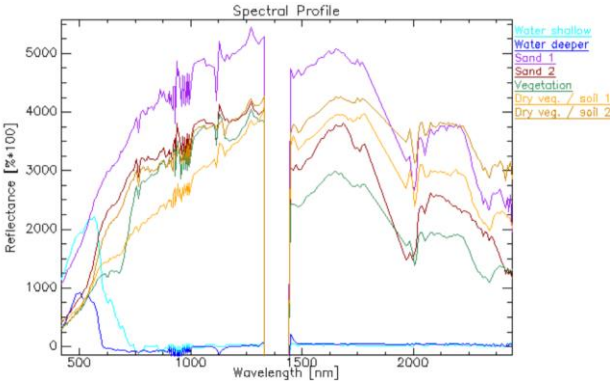

Figure 7-39 DT148217_011, single pixel spectra (L2A land processor)

- **Bogs & forests in western Siberia north of Tomsk, Russia (DT151218, 2025-09-01)**

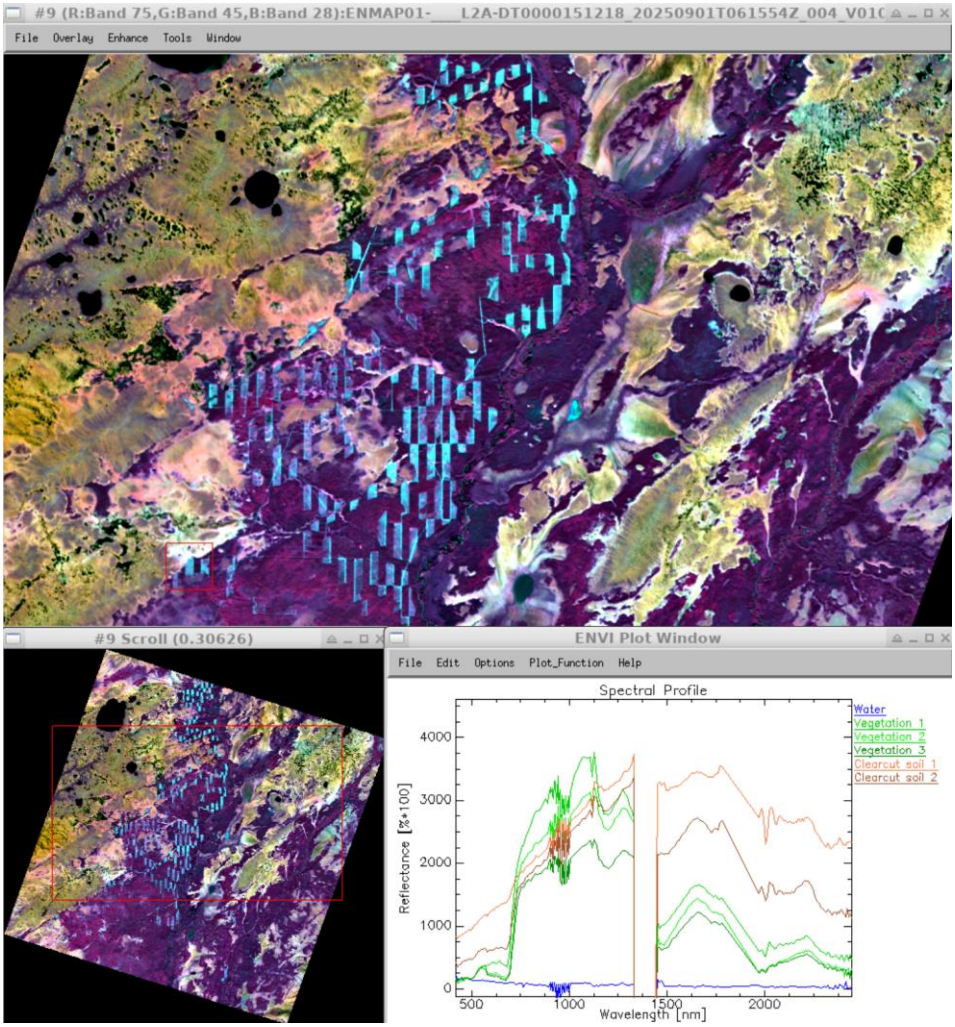

Figure 7-40 DT151218_004, CIR image (nonlinear stretch), and single pixel spectra (L2A land processor).

The forest and bog scene of western Siberia (Figure 7-40) has a variety of surfaces with different levels of moisture, resulting in a colourful impression of the CIR image, and the expected variety of the surface spectra (bottom-right image inlay). Apparent in the scene is a geometrical pattern (in blue in the non-linear CIR stretch), which originates neither in a sensor nor processing defect, but is a feature of the forest management: these almost exactly north-south oriented areas are clear-cuts, showing the typical spectral signatures of soils with some vegetation residuals.

To summarize, the L2A processing is nominal for this scene.

- **Rio Grande dam, US-Mexican border (DT145125, 2025-08-01)**

Checking also a scene of a semi-arid region, the Rio Grande datatake (Figure 7-41) was chosen. The retrieved L2A surface spectra are as expected, showing both the expected spectral features and variability of vital and senescent vegetation, and also the retrieved deep and shallow water spectra are as expected when using the L2A land processor.

For this scene, the L2A processing is also nominal.

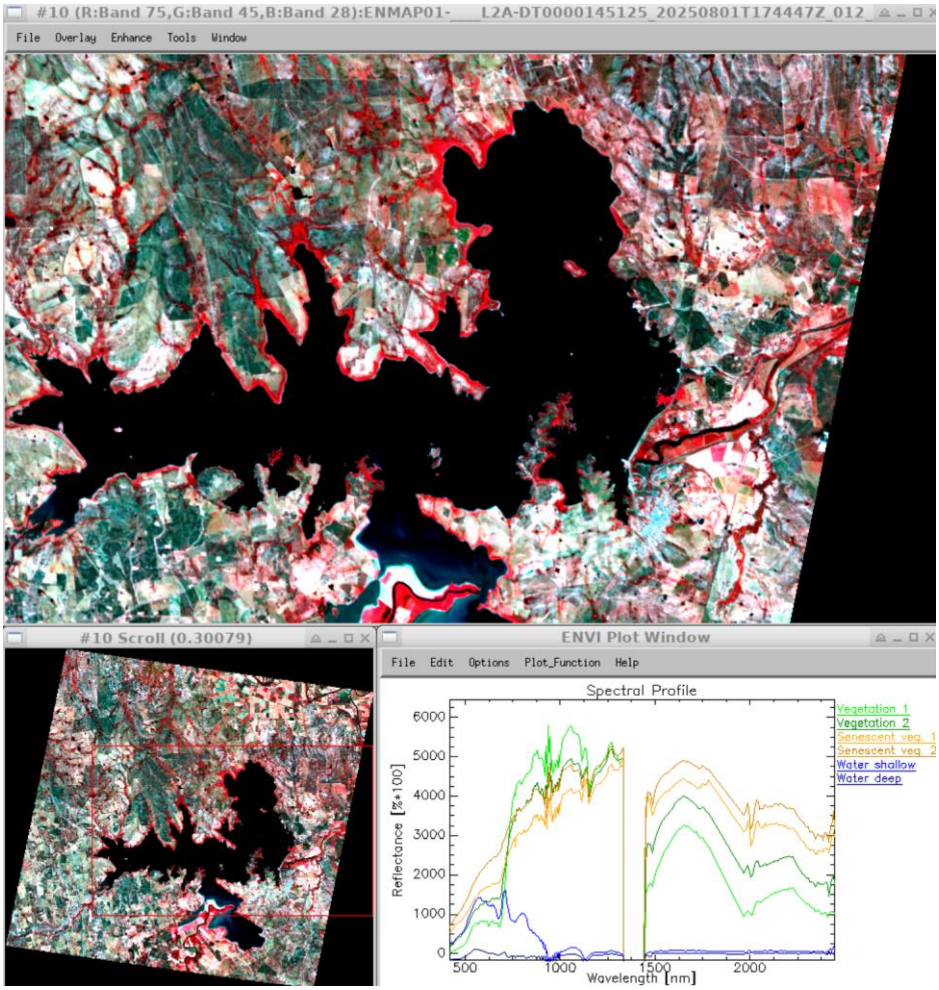

Figure 7-41 DT 145125_012 CIR image (linear stretch), and single pixel spectra (L2A land processor).

8 External Product Validation

The standard quality parameters were validated in the external product validation process for the reporting period. The validation included 109 Level 1B, 182 Level 1C and 114 Level 2A products.

8.1 Level 1B

The following validation scenarios were performed to validate Level 1B products:

- TOA Radiance
- Signal-to-Noise Ratio (SNR)

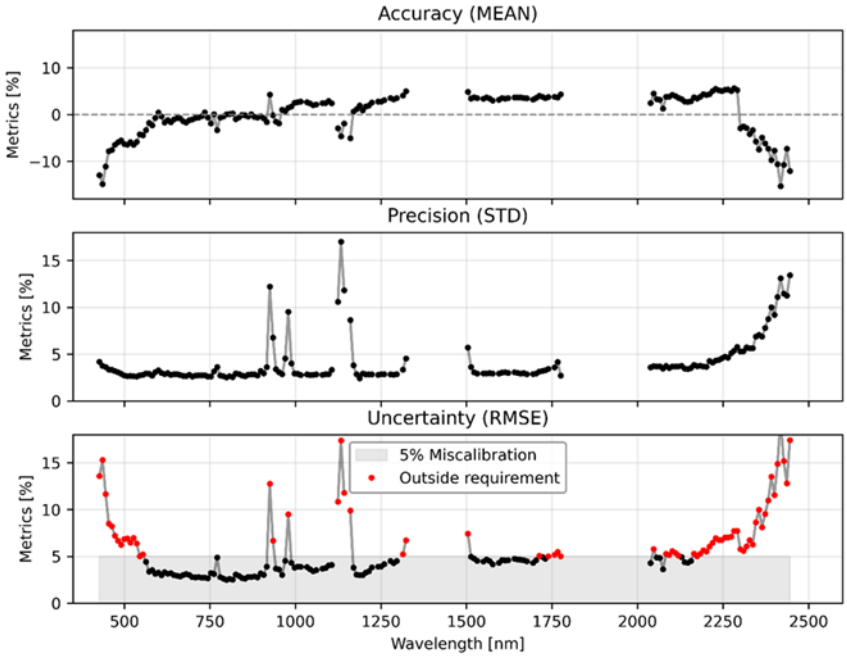

Figure 8-1 Errors between EnMAP TOA radiance and propagated TOA radiance from in situ measurements against wavelength for all arid validation sites based on 33 matchups.

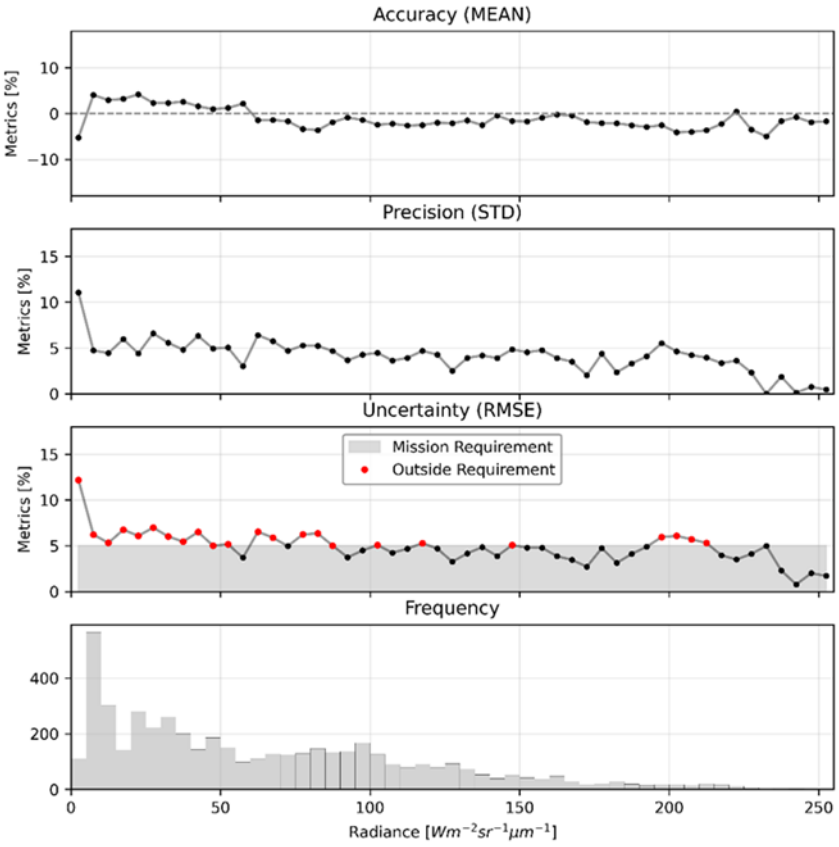

Figure 8-2 Errors between EnMAP TOA radiance and propagated TOA radiance from in situ measurements against radiance level for all arid validation sites based on 33 matchups.

During this validation period, no new EnMAP–in situ matchups could be integrated, as no valid matchups were available either for the RadCalNet sites or from recent in situ data collection campaigns. The RadCalNet site Railroad Valley (RVUS) was preliminarily excluded from the analysis due to pronounced irregular reflectance variations observed in the RadCalNet time series, particularly in the SWIR domain, which could potentially bias the overall validation statistics. These anomalies are suspected to result from variability in surface moisture and evaporitic crust formation, which amplify bidirectional reflectance distribution function (BRDF) effects.

Furthermore, the atmospheric parameters aerosol optical thickness (AOT) and columnar water vapor (CWV) required for the propagation of the in situ reflectance measurements to top-of-atmosphere (TOA) radiance were derived directly from the EnMAP metadata rather than being estimated via least-squares fitting as done previously. While this approach may increase the uncertainty of the propagation, it avoids compensating for potential radiometric calibration differences.

Due to the exclusion of RVUS, the number of available matchups for TOA radiance validation was reduced to 33. However, removing RVUS led to a significant improvement in the TOA radiance validation results across most of the spectral range. In the wavelength interval from 550 to 1300 nm, the relative RMSE is within 3–4 %, which is well inside the mission requirement of 5 %. In the 1500–1750 nm range, RMSE values of around 5 % are observed, placing them at the threshold of the requirement. Slight exceedances (< 7 %) occur in the 2000–2300 nm region, while larger deviations are visible at the detector edges (< 600 nm and > 2300 nm). The largest relative overshoots occur at low radiance levels, which is attributed to the RMSE being normalized by the radiance and therefore being inflated by existing absolute biases.

The SNR assessment was updated based on 206 tiles with the product version 01.05.02 (VNIR 109 and SWIR 97) and was found to be very stable (VNIR: 404:1; SWIR: 260:1) compared to the previous evaluations and inside the mission requirements (VNIR > 343:1 @495 nm SSD 4.7 nm; SWIR > 137:1 @2200 nm & SSD 8.4 nm).

8.2 Level 1C

The following Level 1C validation scenarios have been performed:

- VNIR-to-SWIR spatial co-registration
- Absolute spatial accuracy

The spatial co-registration between VNIR and SWIR has been analyzed for 129 products with the product version 01.05.02. Compared to the previous report, the RMSEs in X and Y direction are slightly lower (5.9 and 6.3 m). Overall, the spatial co-registration performance is stable and well within the mission requirement of less than 30% of a pixel.

The quality of the absolute spatial accuracy is also stable. An RMSE of 10.3 m in X and 12.9 m in Y direction derived from 182 tiles with the product version 01.05.02 was achieved which is well inside the mission requirements (<30 m with GCPs in the image, <100 m without GCPs).

8.3 Level 2A

Land

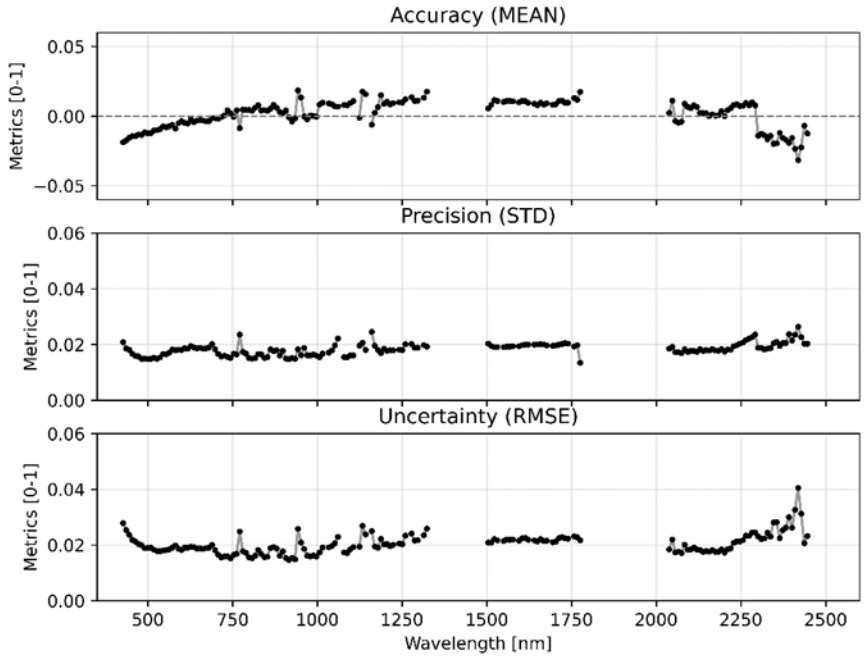

Figure 8-3 Mean difference between BOA reflectance from EnMAP and reference measurements from RadCalNet at Gobabeb against wavelength based on 50 matchups.

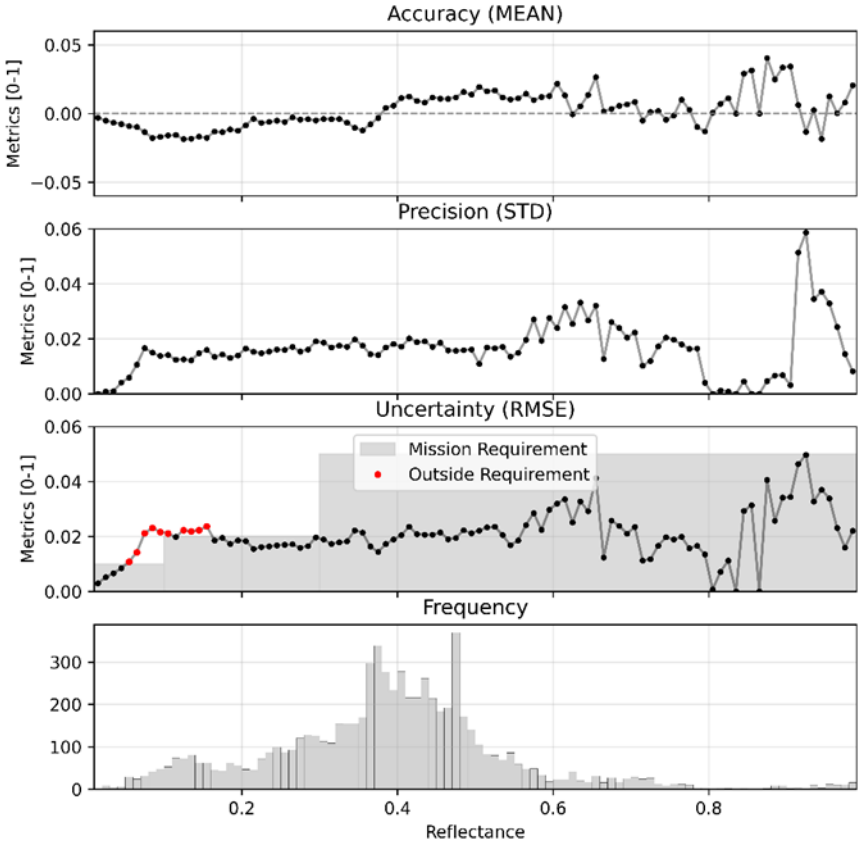

Figure 8-4 Mean difference between BOA reflectance from EnMAP and reference measurements from RadCalNet at Gobabeb against reflectance level based on 50 matchups.

Due to the exclusion of RVUS (see Section 8.1), the number of matchups was lower than in the previous report (50). As in the previous reporting period, the VNIR range yields RMSE values of approximately 1.75-2% reflectance, while in the SWIR range the RMSE is around 2%. Higher residuals, reaching up to 3% RMSE in terms of accuracy and precision, occur at the detector edges, i.e., below 500 nm and above 2400 nm (Figure 8-3). With the exception of very dark targets (reflectance < 20%), the reflectance validation results remain well within the mission requirements (Figure 8-4).

Water

One additional matchup of normalized water-leaving reflectance for Remote Sensing for Trasimeno Lake Observatory (RESTO) was included in the statistical analysis of this report—bringing the total number of analyzed matchups to 64. The new matchup shows uncertainties consistent with those of previous observations. Consequently, the water validation results still show a clear fulfilment of the mission requirements.

8.4 Summary of External Product Monitoring

In general, all validation and quality monitoring during the reporting period indicate that EnMAP product quality is stable and compliant with mission requirements. Local exceedances of the RMSE occur only in the TOA-radiance validation within specific spectral regions. These deviations are likely linked to the reference data and low-radiance conditions in the affected bands and will be monitored in subsequent validation.

9 Others

EnMAP Mission Operations and Status Publications:

No new publications during the reporting period

EnMAP Mission Operations and Status Presentations:

- **IGARSS Brisbane 2025, Brisbane, Australia. August 3 – 8, 2025.**
    - EnMAP – The German Imaging Spectroscopy Spaceborne Mission: New capabilities, processing, and science products 3 years after launch", By S. Chabrillat, Karl Segl, A. Okujeni, S. Asadzadeh, E. Carmona, N. Pinnel, R. Feckl, S. Baur, C. Ong, V. Krieger, M. Bock, L. La Porta
- **76th International Astronautical Congress (IAC 2025), Sydney, Australia, 29 Sep-3 Oct 2025**
    - "EnMAP-PRISMA coordinated multi-mission acquisitions: overview and first outputs", by Patrizia Sacco, Emiliano Carmona, Vera Krieger, Laura La Porta, Nicole Pinnel, Sabine Chabrillat, Karl Segl, Michael Bock, Ettore Lopinto, Giancarlo Varacalli